Hindawi
Journal of Function Spaces
Volume 2022, Article ID 4422186, 19 pages
https://doi.org/10.1155/2022/4422186

Research Article

Effective Analytical Computational Technique for Conformable Time-Fractional Nonlinear Gardner Equation and Cahn-Hilliard Equations of Fourth and Sixth Order Emerging in Dispersive Media

Mohammed Al-Smadi,[1,2,3] **Shrideh Al-Omari**,[4] **Yeliz Karaca**,[5] **and Shaher Momani**[2,6]

[1]*Department of Applied Science, Ajloun College, Al-Balqa Applied University, Ajloun 26816, Jordan*
[2]*Nonlinear Dynamics Research Center (NDRC), Ajman University, Ajman 20550, UAE*
[3]*College of Commerce and Business, Lusail University, Lusail, Qatar*
[4]*Faculty of Engineering Technology, Al-Balqa Applied University, Amman 11134, Jordan*
[5]*University of Massachusetts Medical School, Worcester, MA 01655, USA*
[6]*Department of Mathematics, Faculty of Science, The University of Jordan, Amman 11942, Jordan*

Correspondence should be addressed to Shrideh Al-Omari; shridehalomari@bau.edu.jo

Received 8 July 2022; Accepted 8 September 2022; Published 23 September 2022

Academic Editor: Yusuf Gurefe

The aim of this paper is to investigate the approximate solutions of nonlinear temporal fractional models of Gardner and Cahn-Hilliard equations. The fractional models of the Gardner and Cahn-Hilliard equations play an important role in pulse propagation in dispersive media. The time-fractional derivative is observed in the conformable framework. In this orientation, a reliable computationally algorithm is designed and developed by following a residual error and multivariable power series expansion. Basically, the approximate solutions of pulse wave function of the fractional higher-order Gardner and Cahn-Hilliard equations are obtained in the form of a conformable convergent fractional series. Relevant consequences are theoretically and numerically investigated under the conformable sense. Besides, the analysis of the error and convergence of the developed technique are discussed. Some of the unidirectional homogeneous physical applications of the posed models in a finite compact regime are tested to confirm the theoretical aspects, demonstrate different evolutionary dynamics, and highlight the superiority of the novel developed algorithm compared to other existing analytical methods. For this purpose, associated graphs are displayed in two and three dimensions. Growing and decaying modes of the fractional parameters are analyzed for several α values. From a numerical viewpoint, the simulations and results declare that the proposed iterative algorithm is indeed straightforward and appropriate with efficiency for long-wavelength solutions of nonlinear partial differential equations.

1. Introduction

Nonlinear parabolic partial differential equations are superable mathematical tools for describing different evolutionary dynamics, long-wave propagation, growing and decaying modes, and phase separation of many nonlinear physical system [1–4]. Many applications of nonlinear temporal evolution and phase field models may be obtained from various engineering topics, for instance, cosmology, gravity waves, aerodynamics, blood flow, thermodynamics, incompressible, and inviscid fluid [5–9]. On the other aspect as well, the fractional partial systems play out a significance role in modeling several fascinating nonlinear physical complex systems and realizing the interactions of particles, basic

physics, phase transition, and the process of dynamic that rule such systems. Indeed, they, in the recent past, have been witnessed by scientists owing to its excellent applications in different fields of sciences, including magneto-acoustic propagation in plasma, electromagnetic, chemical kinetics, control theory, quantum mechanics, dissipative systems, gas-solid flows, granular fluids, and hydrodynamics [10–18]. Nevertheless, different types of fractional operators have been moderated by Riemann-Liouville, Atangana-Baleanu, Erdelyi-Kober, Riesz-Caputo, Hadamard, Grünwald-Letnikov, and local-fractional derivatives and conformable. Although the concept of the nonlocal fractional is more acceptable because of the physical long-term features, a deficiency is there as chain, quotient, and Leibniz rules. In this point, the local fractional operators are based on natural generalization of fractional derivatives to avoid the violation of nonnormal rules, keep the local nature of the derivatives, and explore features of certain convergence [19–23].

So long, many effective techniques have been successfully developed and implemented to deal with various categories of temporal fractional nonlinear evolution equations, such as variational iteration method, differential transform method, homotopy perturbation method, reproducing kernel method, operational matrix method, and Galerkin finite element method, in addition to many traveling wave techniques, including $\tan(\phi(\xi)/2)$-expansion method, generalized Kudryashov method, tanh-coth method, and $\exp(-\phi(\epsilon))$ method [24–31]. Finding exact traveling wave, approximate and soliton solutions of higher order temporal fractional partial differential equations in nonlinear wave situations are an issue for knowing the dynamics system of dispersive waves in the phase fields. In this framework, we plan to build approximate and accurate analytical solution for a class of nonlinear homogeneous time-fractional parabolic partial differential equations of higher order equipped with appropriate initial conditions in terms of conformable sense using a novel analytical-computational algorithm. The main contribution lies in designing a superb iteration algorithm to obtain accurate approximate solutions of the posed models in the form of a rapid convergence series at a lower cost of calculations. This algorithm is free of linearization, perturbation, and any restrictive assumptions for handling dispersive and nonlinear terms. To begin with, we consider the following well-known model for the nonlinear third-order time fractional Gardner equation [13, 14]

$$\partial_t^\alpha u + 6\left(u - \lambda^2 u^2\right)u_x + u_{xxx} = 0,\ 0 < \alpha \le 1, \qquad (1)$$

where λ is nontrivial constant parameter, α signifies the order of time-dependent derivatives of fractional order, and $u = u(x, t)$ is wave-profile function scaling spatio-temporal durations of $x \in [a, b]$ and $t \ge 0$. Typically, ∂_t^α represents the variance of u with time and fixed location, and the nonlinear terms uu_x and u^2u_x refer to wave steepening while the linear dispersive term u_{xxx} refers to wave effects. Therefore, it has a vital role regarding interactions of dispersion and nonlinearity in soliton theory. Hereinafter, ∂_t^α stands to the temporal conformable derivative. The aforementioned phase-field model is widely used in several practical applications, such as phase incompressible and inviscid fluids, quantum field theory, curvature flows, quantum mechanics, and gravitational field. Further, it describes a variety of nonlinear wave propagation phenomena in plasma and solid states [13].

In this investigation as well, we focus on the fourth and sixth order time-fractional Cahn-Hilliard equations [24, 25]:

$$\partial_t^\alpha u = \mu u_x + \left(-u_{xx} - u + u^3\right)_{xx},\ 0 < \alpha \le 1, \qquad (2)$$

and

$$\partial_t^\alpha u = \mu u u_x + \left(u_{xx} + u - u^3\right)_{xxxx},\ 0 < \alpha \le 1, \qquad (3)$$

where μ is constant parameter with $\mu \ne 0$. Herein, the nonlinear terms denote the chemical potential of the model, while u_{xxxx} and u_{xxxxxx} denote the dispersive wave effects of the fourth and sixth order system, respectively. This model is profitably used in multiphase incompressible fluid flows, phase ordering dynamics, tumor growth simulation, surface reconstruction, phase separation, image inpainting, spinodal decomposition, and microstructures with elastic inhomogeneity, see [24, 32] for a detailed discussion. Furthermore, the posed models (1)–(3) are involved with initial condition

$$u(x, 0) = f_0(x),\ x \in [a, b], \qquad (4)$$

where $f_0(x)$ is a smooth analytic function of x.

Several types of nonlinear temporal fractional evolution equations have been established in the literature, but several do not assume soliton solutions [33]. Anyhow, the nonlinear time-fractional Gardner and Cahn-Hilliard models are profitably used to describe many nonlinear dispersive wave phenomena arising in nonlinear optics, capillary waves, and plasma physics [34–41]. In [34], nonlocal fourth-order fractional Cahn-Hilliard equation with advection and reaction terms has been considered in the sense of Caputo to investigate the approximate solutions using the homotopy analysis method. Using the new iterative method and q-homotopy analysis method [24], Akinyemi et al. successfully obtained analytical-approximate solutions of the nonlinear fourth and sixth order time-fractional Cahn-Hilliard equations. In [25], homotopy perturbation method has been applied to solve fourth-order Cahn-Hilliard equation with Caputo fractional derivative. Akagi et al. discussed the existence and uniqueness of weak solutions to space-fractional Cahn-Hilliard equation in a bounded domain [35]. Ran and Zhou constructed an implicit difference scheme for the fourth-order time-fractional Cahn-Hilliard equations [36]. In [37], Fourier spectral method has been implemented for time-fractional nonlinear Allen-Cahn and Cahn-Hilliard phase-field models. Prakasha et al. [13] proposed two computational methods for time-fractional Gardner equation and

fourth-order Cahn-Hilliard equation in light of Caputo's concept. Arafa and Elmahdy [38] designed residual power series algorithm to solve fractional nonlinear Gardner and Cahn-Hilliard equations under Caputo sense. Hosseini et al. [39] proposed a new technique based on expansion method for finding exact solutions of time-fractional Conformable Cahn-Hilliard equation. Moreover, Jafari et al. [40] developed the fractional subequation method to construct exact-analytical solutions for fractional Cahn-Hilliard model.

By and large, no conventional approach can be found to produce analytical solutions, soliton solutions, or traveling wave solutions of closed-form for such nonlinear fractional-types dispersive PDEs. So, there have been found demand for sophisticated reliable methods to find analytical and approximate solutions to such problems. This paper formulates an iterative computational algorithm for creating analytical-approximate solutions of a class of nonlinear higher-order time-fractional parabolic partial differential equations by utilizing a novel fractional parameter, the conformable derivative. Estimation of errors for the said algorithm is derived as well. Indeed, several numerical examples have been checked in one-dimensional space to verify the great flexibility and efficiency of the novel developed algorithm, among which the third-order homogeneous time-fractional Gardner equation and fourth and sixth-order homogeneous time-fractional Cahn-Hilliard equations. For this purpose, a comparison study is performed between the presented method and other existing methods. Hereinafter, some notations and auxiliary results are retrieved. In Section 3, an analytical algorithm is expanded to solve nonlinear time-fractional parabolic partial differential equations. In Section 4, certain applications are stated to back up the theoretical concept. Further, several numerical techniques and discussions are reported. In Section 5, some concluding remarks are given.

2. Preliminaries and Principal Results

Fractional calculus has been introduced and developed an interesting tool to explain the memory and characteristics of many processes in a variety of fields of pure and applied science. In recent literature, it has been used to formulate many nonlinear partial differential equation systems and exploited to provide a comprehensive and clear explanation of dynamics, dispersion, wave propagation, and evolutionary models in view of spacetime change. In this direction, different fractional derivatives have been suggested to handle such partial equations like Feller, Riemann-Liouville, Caputo-Fabrizio, Riesz, Grünwald, Mittag-Leffler, and conformable concepts [41–44]. Consequently, the conformable operator has been modified as a natural generalization of the standard notation of derivatives [45]. In this portion, the primary concept of conformable fractional derivative and some interesting properties is highlighted. It also briefly illustrates the concept and characteristics of the residual series expansion under the conformable operator to complete the theoretical aspect of this work.

Definition 1 (see [45]). Given a real-valued function $u(t)$ on $[0,\infty)$, the conformable derivative of $u(t)$ at $\alpha \in (0,1)$ is given by

$$\partial_t^\alpha u(t) = \lim_{\varepsilon \longrightarrow 0} \frac{u\left(t + \varepsilon t^{1-\alpha}\right) - u(t)}{\varepsilon}, t > 0, \tag{5}$$

where $\partial_t^\alpha u(0)$ is understood to mean $\partial_t^\alpha u(0) = \lim_{t \longrightarrow 0^+} \partial_t^\alpha u(t)$.

Definition 2 (see [46]). Given a real-valued function $u(t)$ on $[\mathfrak{z}, \infty)$, if $u(t)$ is α-differentiable; then, the α-fractional integral is given by

$$\mathcal{I}_\mathfrak{z}^\alpha u(t) = \int_\mathfrak{z}^t \frac{u(\xi)}{\xi^{1-\alpha}} d\xi, t > \mathfrak{z} \geq 0, \alpha \in (0,1], \tag{6}$$

provided that the integral is Riemann improper.

The following results are some of the basic characteristics gained in terms of $\partial_t^\alpha u(t)$. For additional properties, we refer to [47–50] and the references therein.

Lemma 3. *Let $\alpha \in (0,1]$ and the functions $v(t)$, $u(t)$ be α-differentiable at a point $t \in [0,\infty)$. Then, for all real constants a_1, a_2, a_3, a_4, the following properties hold:*

(i) $\partial_t^\alpha(e_1 v(t) + e_2 u(t)) = e_1 \partial_t^\alpha v(t) + e_2 \partial_t^\alpha u(t)$

(ii) $\partial_t^\alpha[v(t)u(t)] = v(t)\partial_t^\alpha u(t) + u(t)\partial_t^\alpha v(t)$

(iii) $\partial_t^\alpha[v(t)/u(t)] = (u(t)\partial_t^\alpha v(t) - v(t)\partial_t^\alpha u(t))/u^2(t), u(t) \neq 0$

(iv) $\partial_t^\alpha(t^{a_3}) = a_3 t^{a_3 - \alpha}$

(v) $\partial_t^\alpha(a_4) = 0$

(vi) If $u(t)$ is differentiable, then it also holds that $\partial_t^\alpha u(t) = t^{1-\alpha} du(t)/dt$

Lemma 4 (see [46]). *Given the real-valued functions $u(t)$ and $v(t)$ on $[0,\infty)$, let $\alpha \in (0,1]$, $u(t)$ be first order differentiable and α-differentiable and let $v(t)$ be first order differentiable on the range of $u(t)$. So, the use of the known chain rule yield*

$$\partial_t^\alpha(u \circ v)(t) = t^{1-\alpha} v'(t) u'(v(t)). \tag{7}$$

Definition 5 (see [47]). Given a real-valued function $u(x,t)$ on $[a,b] \times [\mathfrak{z},\infty)$, the αth order conformable partial derivative at a point $t \in [0,\infty)$ is defined as

$$\partial_t^\alpha u(x,t) = \lim_{\varepsilon \longrightarrow 0} \frac{u\left(x, t + \varepsilon(t-\mathfrak{z})^{1-\alpha}\right) - u(x,t)}{\varepsilon}, \alpha \in (0,1]. \tag{8}$$

Definition 6 (see [47]). Given a real-valued function $u(x,t)$ on $[a,b]\times[\vartheta,\infty)$, the αth order conformable integral is defined as

$$\mathcal{J}_{\vartheta}^{\alpha}u(x,t)=\int_{\vartheta}^{t}\frac{u(x,\xi)}{(\xi-\vartheta)^{1-\alpha}}d\xi,\ \alpha\in(0,1]. \tag{9}$$

Definition 7 (see [47]). The fractional series expansion at t_0 can be defined as follows

$$\sum_{i=0}^{\infty}\mathcal{C}_i(x)(t-t_0)^{i\alpha}=\mathcal{C}_0(x)+\mathcal{C}_1(x)(t-t_0)^{\alpha}+\mathcal{C}_2(x)(t-t_0)^{2\alpha}+\cdots,t_0>0, \tag{10}$$

where $\alpha\in(0,1]$, $\mathcal{C}_i(x)$ is the ith unknown coefficient, $t\in[t_0,t_0+\gamma^{1/\alpha})$, $\gamma>0$, and $\gamma^{1/\alpha}$ is the radius of convergence.

Theorem 8 (see [47]). *Given a real-valued function $u(x,t)$ on $[a,b]\times[t_0,t_0+r^{1/\alpha})$, let $u(x,t)$ has many conformable partial derivatives at any point $t\in[0,\infty)$ with the following fractional series expansion at t_0:*

$$u(x,t)=\sum_{i=0}^{\infty}\mathcal{C}_i(x)(t-t_0)^{i\alpha},\alpha>0,t_0>0. \tag{11}$$

Then, $\mathcal{C}_i(x)$, $i=0,1,2,\cdots$, can be calculated by

$$\mathcal{C}_i(x)=\frac{\partial_{t_0}^{i\alpha}u(x,t_0)}{i!\alpha^i}, \tag{12}$$

in which $\partial_{t_0}^{i\alpha}u(x,t_0)$ is the ith conformable partial derivative of $u(x,t)$ about t_0 so that $\partial_{t_0}^{i\alpha}u(x,t_0)=\partial_{t_0}^{\alpha}.\partial_{t_0}^{\alpha}\cdots\partial_{t_0}^{\alpha}u(x,t_0)$ (i-times).

3. Fundamentals of Conformable Fractional Residual Series Approach

Conformable fractional residual series (CFRS) technique is a semianalytic computational algorithm specifically developed to deal with emerging partial differential equations in various nonlinear dynamical phenomena. This technique is based on extending the generalized arbitrary order Taylor series and minimizing the residual errors to detect the unknown compounds. It possesses many attractive and stimulating features and remarkable ability to deal with nonlinear terms profitably without putting any constraints or transformation of the governing models. Consequently, it has gained wide popularity and has recently become an exciting focus of research and a hot tool used in various applied and computational sciences [41–44]. In this portion, a new algorithm is developed to obtain accurate approximate solutions of the nonlinear homogeneous higher-order time-fractional parabolic partial differential equation involving initial conditions in a limited space time domain. In this context, let us see the nonlinear generalized time fractional sixth order partial differential equation as follows

$$\partial_t^{\alpha}u(x,t)+\mathcal{N}\left(u,u^2,u^3,u_x,u_{xx},u_{3x},u_{4x},u_x^2,u_{xx}^2\right)+u_{6x}(x,t)=0,0<\alpha\le1, \tag{13}$$

along with the condition

$$v(x,0)=f_0(x), \tag{14}$$

$x\in[a,b]$, $t\ge0$, α is the order of conformable time-fractional index, $u_{ix}=\partial^i u(x,t)/\partial x^i$, $i=3,4,5,6$, $f_0(x)$ is a given analytical function, and $u(x,t)$ is an unknown sufficiently differentiable wave-profile function. Herein, $\mathcal{N}$ indicates the nonlinear operator from a Banach space $\mathcal{B}$ to itself in terms of uu_x, uu_{xx}^2, $u_x^2u_{xx}$, uu_xu_{3x}, and u^2u_{4x} over a one-dimensional spatiotemporal domain.

Based on the proposed algorithm, the solution $u(x,t)$ of (13) has following form of fractional series expansion at $t_0=0$:

$$u(x,t)=\sum_{i=0}^{\infty}\mathcal{C}_i(x)\frac{t^{i\alpha}}{i!\alpha^i},t\ge t_0, \tag{15}$$

provided that $v(x,0)=\mathcal{C}_0(x)=f_0(x)$. So, the n-term truncated series solution $u_n(x,t)$ of $u(x,t)$ in view of the initial condition (14) can be described as

$$u_n(x,t)=\mathcal{C}_0(x)+\sum_{i=1}^{n}\mathcal{C}_i(x)\frac{t^{i\alpha}}{i!\alpha^i}. \tag{16}$$

Basically, the residual error $\mathcal{R}_{\vartheta}(x,t)$ of model (13) is defined as

$$\mathcal{R}_{\vartheta}(x,t)=\partial_t^{\alpha}u(x,t)+\mathcal{N}\left(u,u^2,u^3,u_x,u_{xx},u_{3x},u_{4x},u_x^2,u_{xx}^2\right)+u_{6x}(x,t), \tag{17}$$

and thus the n-term truncated residual of $\mathcal{R}_{\vartheta}(x,t)$ is expressed by

$$\mathcal{R}_{\vartheta}^{n}(x,t)=\partial_t^{\alpha}u_n(x,t)+\mathcal{N}\left(u_n,u_n^2,\cdots,u_{nxx}^2\right)+u_{n6x}(x,t), \tag{18}$$

where $u_{nkx}=\partial^k u_n(x,t)/\partial_{x^k}$, $\mathcal{R}_{\vartheta}(x,t)=0=\partial_t^{(n-1)\alpha}\mathcal{R}_{\vartheta}(x,t)$, $n=1,2,3,\cdots,x\in[a,b]$, $0\le t<\mathcal{T}$, $\mathcal{T}\equiv t_0+r^{1/\alpha}$, and $\partial_t^{(n-1)\alpha}\mathcal{R}_{\vartheta}^{n}(x,t)_{|t=0}\equiv0$ for each $n=1,2,3,\cdots$.

To demonstrate the main steps of the residual series algorithm in finding out the values of unknown parameters $\mathcal{C}_i(x)$ of the n-term truncated solution (16), set $n=1$ and equate $\mathcal{R}_{\vartheta}^{1}(x,t)$ to zero at $t=0$, so that $\mathcal{C}_1(x)$ can be acquired. Thereafter, by applying the operator ∂_t^{α} on both

Consider the nonlinear generalized time fractional sixth order partial differential equation (13) along with the initial condition (14). Let $u(x,t)$ be a solution of model (13) and (14) that has nth order partial derivatives in conformable sense at any point $t \in [t_0, \mathcal{T})$. Then, to obtain the nth approximation, execute the underlying steps:

Step A. Expand the solution $u(x,t)$ of model (13) about $t_0 = 0$ as follows

$u(x,t) = \sum_{i=0}^{\infty} \mathscr{C}_i(x)(t^{i\alpha}/i!\alpha^i)$, $t \geq t_0$.

Step B. Give a definition of the nth-truncated solution of $u(x,t)$ in view of the initial condition (14) as follows

$u_n(x,t) = \mathscr{C}_0(x) + \sum_{i=1}^{n} \mathscr{C}_i(x)(t^{i\alpha}/i!\alpha^i)$.

Step C. Do truncate the nth residual error of $\mathscr{R}_j(x,t)$ so

$\mathscr{R}_j^n(x,t) = \partial_t^{\alpha} u_n(x,t) + \mathscr{N}(u_n, u_n^2, \cdots, u_{nxx}^2) + u_{n6x}(x,t)$,

where $u_{nkx} = \partial^k u_n(x,t)/\partial_{x^k}$.

Step D. Invoke the series solution obtained in Step B to the nth-truncated residual error obtained in Step C as follows

$\mathscr{R}_j^n(x,t) = \partial_t^{\alpha}(\mathscr{C}_0(x) + \sum_{i=1}^{n} \mathscr{C}_i(x)(t^{i\alpha}/i!\alpha^i)) + \mathscr{N}[(\mathscr{C}_0(x) + \sum_{i=1}^{n} \mathscr{C}_i(x)(t^{i\alpha}/i!\alpha^i)), (\mathscr{C}_0(x) + \sum_{i=1}^{n} \mathscr{C}_i(x)(t^{i\alpha}/i!\alpha^i))^2, \cdots,$
$(\mathscr{C}_0(x) + \sum_{i=1}^{n} \mathscr{C}_i(x)(t^{i\alpha}/i!\alpha^i))_{xx}^2] + (\mathscr{C}_0(x) + \sum_{i=1}^{n} \mathscr{C}_i(x)(t^{i\alpha}/i!\alpha^i))_{6x}$.

Step E. Employ $\partial_t^{(n-1)\alpha}$ for every $n = 1, 2, 3, \cdots$ to the obtained equation in Step D to get

$\partial_t^{(n-1)\alpha}\mathscr{R}_j^m(x,t) = \partial_t^{n\alpha}(\mathscr{C}_0(x) + \sum_{i=1}^{n} \mathscr{C}_i(x)(t^{i\alpha}/i!\alpha^i)) + \partial_t^{(n-1)\alpha}\mathscr{N}[(\mathscr{C}_0(x) + \sum_{i=1}^{n} \mathscr{C}_i(x)(t^{i\alpha}/i!\alpha^i)),$
$(\mathscr{C}_0(x) + \sum_{i=1}^{n} \mathscr{C}_i(x)(t^{i\alpha}/i!\alpha^i))^2, \cdots, (\mathscr{C}_0(x) + \sum_{i=1}^{n} \mathscr{C}_i(x)(t^{i\alpha}/i!\alpha^i))_{xx}^2] + \partial_t^{(n-1)\alpha}(\mathscr{C}_0(x) + \sum_{i=1}^{n} \mathscr{C}_i(x)(t^{i\alpha}/i!\alpha^i))_{6x}$.

Step F. To obtain the first few terms for $\mathscr{C}_i(x)$ with the aid of $\partial_t^{(n-1)\alpha}\mathscr{R}_j^n(x,0) = 0$ execute the following subroutine:

F1. In Step E, put n=1, compute $\mathscr{R}_j^1(x,t)$ and find solution for $\mathscr{R}_j^1(x,0) = 0$ to get $\mathscr{C}_1(x)$.

F2. Once again, in Step E, set n=2, compute $\partial_t^{\alpha}\mathscr{R}_j^2(x,t)$ and find solution for $\partial_t^{\alpha}\mathscr{R}_j^2(x,0) = 0$ to get $\mathscr{C}_2(x)$.

F3. Once again, n Step E, set $n = 3$, compute $\partial_t^{2\alpha}\mathscr{R}_j^3(x,t)$ and find solution for $\partial_t^{2\alpha}\mathscr{R}_j^3(x,0) = 0$ to get $\mathscr{C}_3(x)$.

F4. Proceed for arbitrary order k by setting $n = k$, computing $\partial_t^{(k-1)\alpha}\mathscr{R}_j^k(x,t)$, and establishing the new equation $\partial_t^{(k-1)\alpha}\mathscr{R}_j^k(x,0) = 0$ to get the kth coefficients $\mathscr{C}_k(x)$.

Step G. Keep the new components in an infinite series form. In fact, the closed form of the solution can be established in such way, that is, $u(x,t) = \lim_{k \longrightarrow \infty} u_k(x,t)$, if the relation of the pattern is very regular. If it was not the case, the solutions $u_k(x,t)$ can be approximately obtained. Then, Stop.

Algorithm 1

sides of the resulting relevant equation for $n = 2$, and solving $\partial_t^{\alpha}\mathscr{R}_j^2(x,0) = 0$, the coefficient $\mathscr{C}_2(x)$ can be acquired as well. Continuing likewise, the rest of coefficients $\mathscr{C}_i(x)$ for each $i \geq 3$ of the fractional series expansion (16) can be acquired. To complete the presentation and clarification, the underlying algorithm is dedicated.

Lemma 9. *Let $u(x,t)$ be the solution of PDEs (13) and (14) that has nth order partial derivatives in conformable sense at any point $t \in [t_0, t_0 + r^{1/\alpha})$ and the fractional expansion of equation (15) at $t_0 = 0$. If there exist $\eta(x) > 0$ so that $|\partial_t^{(n+1)\alpha}u(x,\xi)| \leq \eta(x)$ for all $0 < \xi < t$, then, the remainder term holds the underlying inequality*

$$|\mathscr{P}_k(x,t)| \leq \frac{\eta(x)}{(n+1)!\alpha^{n+1}} t^{(n+1)\alpha}, \tag{19}$$

in which $\mathscr{P}_k(x,t) = \sum_{k=n+1}^{\infty}(\partial_t^{k\alpha}u(x,\xi)/\alpha^k k!)t^{k\alpha}$.

Corollary 10. *Let $u(x,t)$ and $u_n(x,t)$ be respectively the analytic and approximate solutions of PDEs (13) and (14). If there exists $\xi \in [0,1]$ so that $\|u_{n+1}(x,t)\| \leq \xi\|u_n(x,t)\|$ for each $(x,t) \in [a,b] \times [t_0, \mathcal{T})$, and $\|f_0(x)\| < \infty$ for $x \in [a,b]$. Then, $u_n(x,t)$ converges to $u(x,t)$ as soon as $n \longrightarrow \infty$.*

Proof. Since $\|u_{n+1}(x,t)\| \leq \xi\|u_n(x,t)\|$ for each $(x,t) \in [a,b] \times [t_0, \mathcal{T})$, then, $\|u_1(x,t)\| \leq \xi\|u_0(x,t)\| = \xi\|f_0(x)\|$, and then, $\|u_2(x,t)\| \leq \xi^2\|f_0(x)\|$. Subsequently, we have $\|u_n(x,t)\| \leq \xi^n\|f_0(x)\|$. This leads to $\sum_{k=n+1}^{\infty}\|u_k(x,t)\| \leq \|f_0(x)\|\sum_{k=n+1}^{\infty}\lambda^k$. Thus, it can be observed that

$$\begin{aligned} \|u(x,t) - u_n(x,t)\| &= \left\| \sum_{k=n+1}^{\infty} u_k(x,t) \right\| \\ &\leq \sum_{k=n+1}^{\infty} \|u_k(x,t)\| \\ &\leq \sum_{k=n+1}^{\infty} \lambda^k \|f_0(x)\| \\ &= \frac{\lambda^{n+1}}{1-\lambda}\|f_0(x)\| \longrightarrow 0 \text{ for } n \longrightarrow \infty. \end{aligned} \tag{20}$$

□

4. Numerical Experiments and Discussion

Temporal fractional evolution equations are efficient approaches for modeling nonlinear waves and knowing the basic physics, phase separation properties, and evolutionary dynamics that govern these equations. The fractional Gardner and Cahn-Hilliard equations are unidirectional temporal

nonlinear parabolic partial differential equations, describe nonlinear wave propagation phenomena, and phase-field separation models [13, 24]. It balances the dispersion and nonlinearity effects of the soliton dynamics. In this portion, the conformable power series algorithm in view of the residual error functions is applied to solve the homogeneous third-order time-fractional Gardner equation as well as the homogeneous fourth and sixth-order time-fractional Cahn-Hilliard equations, which are very common species of higher-order fractional temporal evolution. The simulation of such models is investigated as well. More representative results are introduced with physical interpretations for various fractional parameters to hold up the theoretical framework and produce visualization of wave function behavior. Moreover, different comparisons are produced to justify the effect of our new method. Calculations are performed by Mathematica 12.2 computing system [51].

4.1. Solution of Nonlinear Third-Order Fractional Gardner Equation. The one-dimensional nonlinear third-order fractional Gardner equation (FGE) considered in this portion can be presented in view of the conformable time derivative as follows [13, 14]:

$$\partial_t^\alpha u = -6\left(u - \lambda^2 u^2\right)u_x - u_{xxx}, 0 < \alpha \le 1, \tag{21}$$

along with the underlying initial condition

$$u(x,0) = \frac{1}{2} + \frac{1}{2}\tanh\left(\frac{x}{2}\right), \tag{22}$$

where λ is constant, $\lambda \neq 0$, $x \in [a, \ell]$, $t \ge 0$, $u = u(x,t)$ is a sufficiently differentiable function representing the wave-profile scaling spatiotemporal duration of wave propagation in dispersed media. Typically, the nonlinear terms in this model refer to wave steepening, and u_{xxx} refers to wave scattering. The aforementioned equation defines an indispensable model for different nonlinear physical applications in plasma, surface tension, hydrodynamics, etc. [14]. The exact solution of the posed model when $\alpha = 1$ and $\lambda = 1$ is given by

$$u(x,t) = \frac{1}{2} + \frac{1}{2}\tanh\left(\frac{x-t}{2}\right). \tag{23}$$

According the CFRS algorithm, the fractional series solution $u(x,t)$ of the FGE (21) about $t = 0$ can be established as follows

$$u(x,t) = \sum_{i=0}^{\infty} \mathscr{C}_i(x)\frac{t^{i\alpha}}{\alpha^i i!}, \tag{24}$$

provided that $\mathscr{C}_0(x) = u(x,0) = 1/2(1 + \tanh(x/2))$. Subsequently, the nth fractional series $u_n(x,t)$ in view of the initial condition (22) can be truncated as follows

$$u_n(x,t) = \frac{1}{2} + \frac{1}{2}\tanh\left(\frac{x}{2}\right) + \sum_{i=1}^{n} \mathscr{C}_i(x)\frac{t^{i\alpha}}{\alpha^i i!}, \tag{25}$$

and the residual error function $\mathscr{R}_\jmath(x,t)$ can be expressed as

$$\mathscr{R}_\jmath(x,t) = \partial_t^\alpha u + 6\left(u - \lambda^2 u^2\right)u_x + u_{xxx}, 0 < \alpha \le 1, \tag{26}$$

in which $\mathscr{R}_\jmath(x,t) = 0 = \partial_t^{(n-1)\alpha}\mathscr{R}_\jmath(x,t)$, $n = 1, 2, 3, \cdots$, for each $x \in [a, \ell]$ and $t \ge 0$.

In this direction as well, the nth truncated error $\mathscr{R}_\jmath^n(x,t)$ of $\mathscr{R}_\jmath(x,t)$ can be expressed as

$$\mathscr{R}_\jmath^n(x,t) = \partial_t^\alpha u_n + 6\left(u_n - \lambda^2 u_n^2\right)u_{nx} + u_{nxxx}, \tag{27}$$

provided that $\mathscr{R}_\jmath^n(x,t) \longrightarrow \mathscr{R}_\jmath(x,t)$ as $n \longrightarrow \infty$, and $\partial_t^{(n-1)\alpha}\mathscr{R}_\jmath^n(x,t)_{|t=0} \equiv 0$ for each $n = 1, 2, 3, \cdots$.

By viewing the representation of the truncated series (25) and minimizing the residual error (27) of the governing equation, the unknown coefficients $\mathscr{C}_i(x)$ can be computed for each value of $i = 1, 2, \cdots, n$ in order to obtain the nth approximate solution $u_n(x,t)$. To begin with, the first fractional series solution at $n = 1$ assumes the form

$$u_1(x,t) = \frac{1}{2} + \frac{1}{2}\tanh\left(\frac{x}{2}\right) + \frac{1}{\alpha}\mathscr{C}_1(x)t^\alpha, \tag{28}$$

as well as the first residual function assumes the form

$$\mathscr{R}_\jmath^1(x,t) = \partial_t^\alpha u_1 + 6\left(u_1 - \lambda^2 u_1^2\right)u_{1x} + u_{1xxx}. \tag{29}$$

Consequently, putting $u_1(x,t)$ into $\mathscr{R}_\jmath^1(x,t)$ to get

$$\begin{aligned}\mathscr{R}_\jmath^1(x,t) = {} & \mathscr{C}_1(x) + \frac{6}{\alpha^3}\left(\alpha\mathscr{C}_0(x) + \mathscr{C}_1(x)t^\alpha\right) \\ & \cdot \left(\alpha\mathscr{C}_0'(x) + \mathscr{C}_1'(x)t^\alpha\right) \\ & \cdot \left(\alpha - \lambda^2\left(\alpha\mathscr{C}_0(x) + \mathscr{C}_1(x)t^\alpha\right)\right) \\ & + \frac{1}{\alpha}\left(\alpha\mathscr{C}_0^{(3)}(x) + \mathscr{C}_1^{(3)}(x)t^\alpha\right).\end{aligned} \tag{30}$$

Herein, with the aid of $\mathscr{R}_\jmath^1(x,t)_{|t=0} = 0$, it yields

$$\mathscr{C}_1(x) + 6\mathscr{C}_0(x)\left(1 - \lambda^2\mathscr{C}_0(x)\right)\mathscr{C}_0'(x) + \mathscr{C}_0^{(3)}(x) = 0, \tag{31}$$

which implies

$$\begin{aligned}\mathscr{C}_1(x) = {} & -\frac{1}{8}\left(1 + \left(4 - 3\lambda^2\right)\cosh(x) + 3\left(1 - \lambda^2\right)\sinh(x)\right) \\ & \cdot \operatorname{sech}^4\left(\frac{x}{2}\right).\end{aligned} \tag{32}$$

Hence, the first series solution $u_1(x,t)$ can be read as

$$u_1(x,t) = \frac{1}{2} + \frac{1}{2}\tanh\left(\frac{x}{2}\right) - \frac{1}{8\alpha}\left(1 + \left(4 - 3\lambda^2\right)\cosh(x) + 3\left(1-\lambda^2\right)\sinh(x)\right) \cdot \operatorname{sech}^4\left(\frac{x}{2}\right)t^{\alpha}. \tag{33}$$

Sequentially, the second truncated series $u_2(x,t)$ can be computed for $n = 2$ in (27) such that

$$\mathscr{R}_j^2(x,t) = \partial_t^{\alpha}u_2 + 6\left(u_2 - \lambda^2 u_2^2\right)u_{2x} + u_{2xxx}, \tag{34}$$

where $u_2(x,t) = u_1(x,t) + (1/2\alpha^2)\mathscr{C}_2(x)t^{2\alpha}$. By employing the conformable operator ∂_t^{α} on both sides of equation (34), we get that

$$\partial_t^{\alpha}\mathscr{R}_j^2(x,t) = \mathscr{C}_2(x) + 6\partial_t^{\alpha}\left(u_2 - \lambda^2 u_2^2\right)u_{2x} + \frac{1}{\alpha}\left(\mathscr{C}_1^{(3)}(x) + \mathscr{C}_2^{(3)}(x)t^{\alpha}\right). \tag{35}$$

Consequently, solving the term $\partial_t^{\alpha}\mathscr{R}_j^2(x,t)_{|t=0} = 0$ in the aforementioned equation with the help of Mathematica's symbolic architecture [51] leads to

$$\begin{aligned}\mathscr{C}_2(x) = -\frac{1}{64}\operatorname{sech}^7\left(\frac{x}{2}\right)\Bigg(&24\left(1-\lambda^2\right)\cosh\left(\frac{x}{2}\right) - 6\left(22 - 37\lambda^2 + 15\lambda^4\right)\cosh\left(\frac{3x}{2}\right) \\ &+ \left(24 - 42\lambda^2 + 18\lambda^4\right)\cosh\left(\frac{5x}{2}\right) + \left(206 - 204\lambda^2\right)\sinh\left(\frac{x}{2}\right) \\ &- \left(129 - 222\lambda^2 + 90\lambda^4\right)\sinh\left(\frac{3x}{2}\right) \\ &+ \left(25 - 42\lambda^2 + 18\lambda^4\right)\sinh\left(\frac{5x}{2}\right)\Bigg).\end{aligned} \tag{36}$$

Hence, the solution $u_2(x,t)$ can be given as

$$\begin{aligned}u_2(x,t) = \frac{1}{2} + \frac{1}{2}\tanh\left(\frac{x}{2}\right) - \frac{1}{8\alpha}\left(1 + \left(4 - 3\lambda^2\right)\cosh(x)\right. &\\ \left. + 3\left(1-\lambda^2\right)\sinh(x)\right)\operatorname{sech}^4\left(\frac{x}{2}\right)t^{\alpha} &\\ - \frac{1}{128\alpha^2}\operatorname{sech}^7\left(\frac{x}{2}\right)\Bigg(24\left(1-\lambda^2\right)\cosh\left(\frac{x}{2}\right) &\\ - 6\left(22 - 37\lambda^2 + 15\lambda^4\right)\cosh\left(\frac{3x}{2}\right) &\\ + \left(24 - 42\lambda^2 + 18\lambda^4\right)\cosh\left(\frac{5x}{2}\right) &\\ + \left(206 - 204\lambda^2\right)\sinh\left(\frac{x}{2}\right) &\\ - \left(129 - 222\lambda^2 + 90\lambda^4\right)\sinh\left(\frac{3x}{2}\right) &\\ + \left(25 - 42\lambda^2 + 18\lambda^4\right)\sinh\left(\frac{5x}{2}\right)\Bigg)t^{2\alpha}.\end{aligned} \tag{37}$$

Continuing in this manner, the truncated series $u_3(x,t)$ of the series expansion (25) may be computed by applying $n = 3$ in (27), allowing $\partial_t^{2\alpha}$ to act on both sides of the new relevant equation then establishing $\partial^{2\alpha}\mathscr{R}_j^3(x,t)/\partial t^2{}_{|t=0} = 0$ with the aid of Mathematica. To finish our process, we can assume that $u_2(x,t)$ is our approximate solution of the FGE (21) along with condition (22). Moreover, the values of $\mathscr{C}_n(x)$ for each $n \geq 3$ may be counted likewise. In what follows, the achieved n terms in the form of an infinite series leads to the solution $u(x,t)$ of the FGEs (21)–(22). Especially, the solution of FGEs (21) and (22) at $\alpha = 1$ and $\lambda = 1$ can be written in the form

$$\begin{aligned}u(x,t) = \frac{1}{2} + \frac{1}{2}\tanh\left(\frac{x}{2}\right) - \frac{1}{4}\operatorname{sech}^2\left(\frac{x}{2}\right)t &\\ - \operatorname{csch}^3(x)\sinh^4\left(\frac{x}{2}\right)t^2 &\\ + \frac{1}{48}(2 - \cosh(x))\operatorname{sech}^4\left(\frac{x}{2}\right)t^3 &\\ - \frac{1}{384}\left(\sinh\left(\frac{3x}{2}\right) - 11\sinh\left(\frac{x}{2}\right)\right) &\\ \cdot \operatorname{sech}^5\left(\frac{x}{2}\right)t^4 + \cdots,\end{aligned} \tag{38}$$

which agrees with the analytical solution acquired by q-homotopy analysis transform method (q-HATM), fractional natural decomposition method (FNDM) [13], and q-homotopy analysis method (q-HAM) [14], so that

$$u(x,t) = \frac{1}{2} + \frac{1}{2}\tanh\left(\frac{x-t}{2}\right). \tag{39}$$

In what follows, some graphic representations achieved by the presented algorithm for FGEs (21) and (22) are displayed in Figures 1 and 2. At lease three-dimensional surface plots of the exact solution whereas the fourth approximate solution are depicted in Figure 1 for diverse values of α with $\lambda = 1$ over a large enough spatio temporal domain $[-20, 20] \times [0, 3]$. In Figure 2, the moving and evolutionary dynamics of fractional wave function of FGEs (21) and (22) are provided in 2D graph over $[-10, 10]$ versus t at $\lambda = 1$ based on different values of α that are given as $\alpha = 1$, 0.75, 0.5, and 0.25, respectively. From these graphs, it can be observed the tremendous influence of the fractional parameters α on the solutions' consistency with respect to the time t. By measuring the absolute error $|u - u_3|$, the achieved numerical solutions of FGEs (21) and (22) are given in Table 1 for distinct values of x and fixed $t = 0.2$ when $\alpha = 1$ and $\lambda = 1$ and compared with absolute errors obtained in [13] as well. The efficiency of our method is straightforward from these

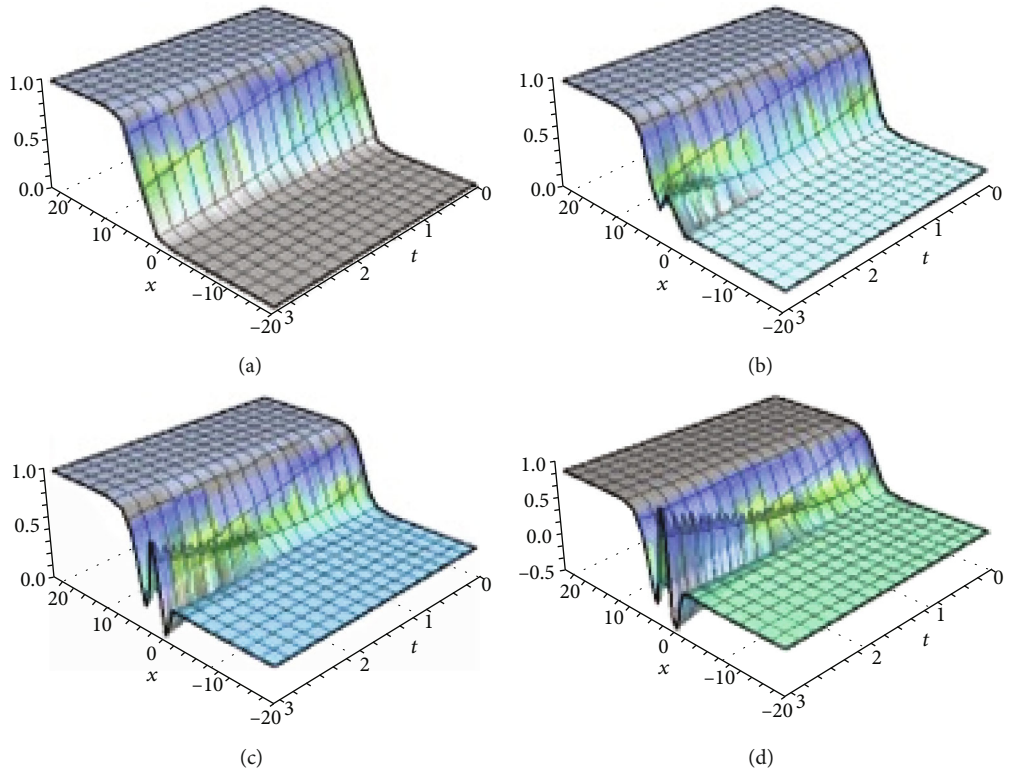

Figure 1: Surface wave behavior of $u_4(x,t)$ of FGEs (21) and (22) with $\lambda = 1$ for diverse α: (a) exact, (b) $\alpha = 0.75$, (c) $\alpha = 0.5$, and (d) $\alpha = 0.25$.

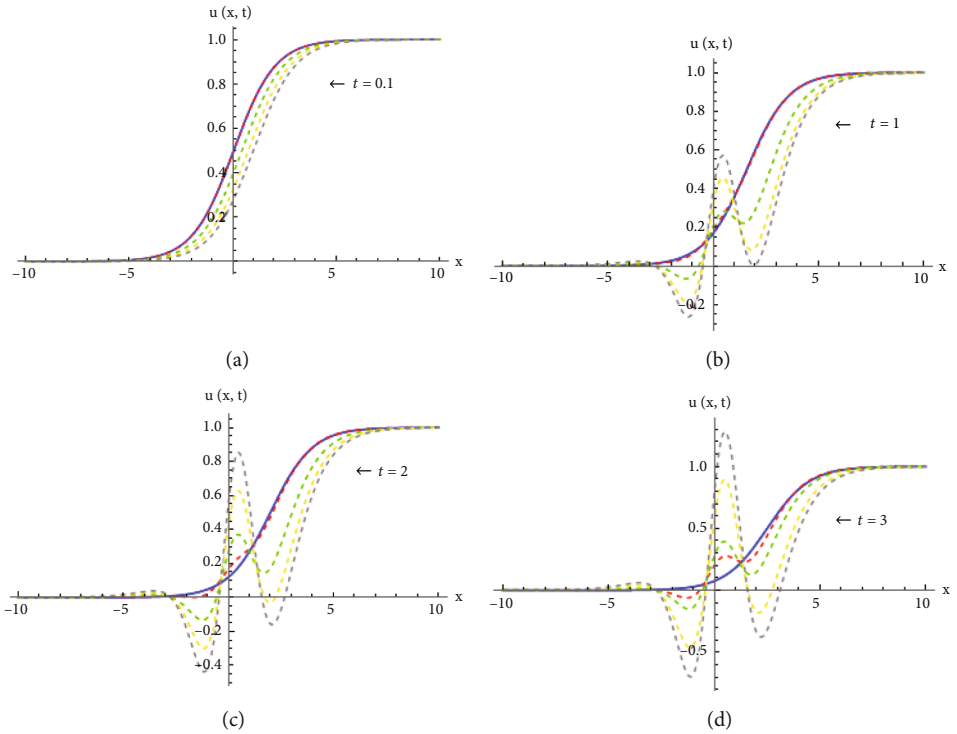

Figure 2: Elevation of wave surface of $u_4(x,t)$ of FGEs (21) and (22) with $\lambda = 1$ and fixed t for various values of α, in which exact blue, $\alpha = 1$ red, $\alpha = 0.75$ green, $\alpha = 0.5$ yellow, and $\alpha = 0.25$ gray.

Table 1: Comparison of numerical outcomes for FGEs (21) and (22) with = 0.2,$\alpha = 1$, and $\lambda = 1$.

x_i	$u(x,t)$	$u_3(x,t)$	$\lvert u - u_3\rvert$	$\lvert u - u_3\rvert\lvert u\rvert^{-1}$	FNDM [13]	q-HATM [13]
0.1	0.475021	0.475020	9.95627×10^{-7}	2.09596×10^{-6}	9.95627×10^{-7}	9.95627×10^{-7}
0.2	0.500000	0.499997	2.61331×10^{-6}	5.22661×10^{-6}	2.61331×10^{-6}	2.61331×10^{-6}
0.3	0.524979	0.524975	4.12217×10^{-6}	7.85207×10^{-6}	4.12217×10^{-6}	4.12217×10^{-6}
0.4	0.549834	0.549829	5.46303×10^{-6}	9.93579×10^{-6}	5.46303×10^{-6}	5.46303×10^{-6}
0.5	0.574443	0.574436	6.58827×10^{-6}	1.14690×10^{-5}	6.58827×10^{-6}	6.58827×10^{-6}

Table 2: Absolute errors $\lvert u - u_3\rvert$ for different values of fractional order α at $t = 0.2, \lambda = 1$ of FGEs (21) and (22).

x_i	$\alpha = 1$	$\alpha = 0.95$	$\alpha = 0.75$	$\alpha = 0.5$	$\alpha = 0.25$
0.1	9.95627×10^{-7}	1.33546×10^{-6}	3.56984×10^{-6}	8.10067×10^{-6}	2.05633×10^{-5}
0.2	2.61331×10^{-6}	3.01435×10^{-6}	5.77678×10^{-6}	3.93725×10^{-5}	1.30242×10^{-4}
0.3	4.12217×10^{-6}	5.86542×10^{-6}	2.67443×10^{-5}	3.11823×10^{-5}	1.65983×10^{-4}
0.4	5.46303×10^{-6}	6.13259×10^{-6}	3.87654×10^{-5}	1.92139×10^{-4}	3.65432×10^{-4}
0.5	6.58827×10^{-6}	8.43010×10^{-6}	1.65438×10^{-5}	1.00045×10^{-4}	3.76543×10^{-4}

results. Moreover, Table 2 provides the absolute errors between the exact solutions and the third approximate solutions of FGEs (21) and(22) for different values of fractional order α such as $\alpha = \{1, 0.95, 0.75, 0.5, 0.25\}$ at $t = 0.2$ and $\lambda = 1$. These results show good agreement between the solutions when the fractional values differ.

4.2. Solution of Nonlinear Fourth-Order Time-Fractional Cahn-Hilliard Equation. The one-dimensional nonlinear fourth-order fractional Cahn-Hilliard (FCH4) equation considered in this portion can be presented in terms of the conformable time derivative as follows [24, 25]:

$$\partial_t^\alpha u = \mu u_x + 6uu_x^2 + \left(3u^2 - 1\right)u_{xx} - u_{xxxx}, 0 < \alpha \le 1, \tag{40}$$

along with the underlying initial condition

$$u(x,0) = \tanh\left(\frac{x}{\sqrt{2}}\right), \tag{41}$$

where μ is aconstant, $\mu \neq 0$, $x \in [a, b]$, $t \ge 0$, $u = u(x,t)$ is sufficiently differentiable function representing the wave-profile scaling spatiotemporal duration of wave propagation in dispersed media. Herein, the nonlinear terms in this model refer to chemical potential dynamics, and u_{xxxx} refers to wave scattering. This equation has various applications in topology optimization, surface reconstruction, phase separation, phase ordering dynamics, magneto-acoustic propagation in plasma, multiphase incompressible fluid flows, image inpainting, and so forth [25, 32]. The exact solution of the posed model when $\alpha = 1$ and $\mu = 1$ is given by

$$u(x,t) = \tanh\left(\frac{x + t}{\sqrt{2}}\right). \tag{42}$$

By performing the CFRS algorithm, the fractional series solution $u(x,t)$ of the FCH4 equation (40) about $t = 0$ can be constructed as follows

$$u(x,t) = \sum_{i=0}^{\infty} \mathscr{C}_i(x)\frac{t^{i\alpha}}{\alpha^i i!}, \tag{43}$$

provided that $\mathscr{C}_0(x) = u(x,0) = \tanh(x/\sqrt{2})$. Subsequently, the nth fractional series $u_n(x,t)$ in view of the initial condition (41) can be truncated by

$$u_n(x,t) = \tanh\left(\frac{x}{\sqrt{2}}\right) + \sum_{i=1}^{n} \mathscr{C}_i(x)\frac{t^{i\alpha}}{\alpha^i i!}, \tag{44}$$

and the error function $\mathscr{R}_j(x,t)$ can be expressed as

$$\begin{aligned}\mathscr{R}_j(x,t) = \partial_t^\alpha u - \mu u_x - 6uu_x^2 - \left(3u^2 - 1\right)u_{xx} \\ + u_{xxxx}, 0 < \alpha \le 1,\end{aligned} \tag{45}$$

in which $\mathscr{R}_j(x,t) = 0 = \partial_t^{(n-1)\alpha}\mathscr{R}_j(x,t)$, $n = 1, 2, 3, \cdots$, for each $x \in [a, b]$ and $t \ge 0$.

In this orientation as well, the nth truncated error $\mathscr{R}_j^n(x,t)$ of $\mathscr{R}_j(x,t)$ can be expressed as

$$\begin{aligned}\mathscr{R}_j^n(x,t) = \partial_t^\alpha u_n - \mu u_{nx} - 6u_n u_{nx}^2 \\ - \left(3u_n^2 - 1\right)u_{nxx} + u_{nxxxx},\end{aligned} \tag{46}$$

provided that $\mathscr{R}_j^n(x,t) \longrightarrow \mathscr{R}_j(x,t)$ as $n \longrightarrow \infty$, and $\partial_t^{(n-1)\alpha}\mathscr{R}_j^n(x,t)_{|t=0} \equiv 0$ for each $n = 1, 2, 3, \cdots$.

By viewing the representation of the truncated series (44) and minimizing the residual error (46) of the governing equation, the unknown coefficients $\mathscr{C}_i(x)$ can be computed for each value of $i = 1, 2, \cdots, n$ in order to obtain the nth

approximate solution $u_n(x,t)$. To begin with, the first fractional series solution at $n=1$ has the form

$$u_1(x,t)=\tanh\left(\frac{x}{\sqrt{2}}\right)+\frac{1}{\alpha}\mathscr{C}_1(x)t^{\alpha}, \tag{47}$$

as well as the first residual function has the form

$$\begin{aligned}\mathscr{R}_j^1(x,t)&=\partial_t^{\alpha}u_1-\mu u_{1x}-6u_1u_{1x}^2\\&\quad-\left(3u_1^2-1\right)u_{1xx}+u_{1xxxx}.\end{aligned} \tag{48}$$

Consequently, putting $u_1(x,t)$ into $\mathscr{R}_j^1(x,t)$ to get

$$\begin{aligned}\mathscr{R}_j^1(x,t)&=\mathscr{C}_1(x)-\mu\left(\mathscr{C}_0'(x)+\mathscr{C}_1'(x)\frac{t^{\alpha}}{\alpha}\right)\\&\quad-\frac{3(\alpha\mathscr{C}_0(x)+\mathscr{C}_1(x)t^{\alpha})}{\alpha^3}\\&\quad\cdot\left(2\left(\alpha\mathscr{C}_0'(x)+\mathscr{C}_1'(x)t^{\alpha}\right)^2\right.\\&\quad\left.+(\alpha\mathscr{C}_0(x)+\mathscr{C}_1(x)t^{\alpha})\left(\alpha\mathscr{C}_0''(x)+\mathscr{C}_1''(x)t^{\alpha}\right)\right)\\&\quad+\mathscr{C}_0''(x)+\mathscr{C}_1''(x)\frac{t^{\alpha}}{\alpha}+\left(\mathscr{C}_0^{(4)}(x)+\mathscr{C}_1^{(4)}(x)\frac{t^{\alpha}}{\alpha}\right).\end{aligned} \tag{49}$$

Hence, by using $\mathscr{R}_j^1(x,t)_{|t=0}=0$, it yields

$$\begin{aligned}&\mathscr{C}_1(x)-\mu\mathscr{C}_0'(x)-6\mathscr{C}_0(x)\mathscr{C}_0'(x)^2+\mathscr{C}_0''(x)\\&\quad-3\mathscr{C}_0''(x)\mathscr{C}_0(x)^2+\mathscr{C}_0^{(4)}(x)=0,\end{aligned} \tag{50}$$

which yields

$$\mathscr{C}_1(x)=\frac{\mu}{\sqrt{2}}\operatorname{sech}^2\left(\frac{x}{\sqrt{2}}\right). \tag{51}$$

Hence, the solution $u_1(x,t)$ is obtained as

$$u_1(x,t)=\tanh\left(\frac{x}{\sqrt{2}}\right)+\frac{\mu}{\sqrt{2}\alpha}\operatorname{sech}^2\left(\frac{x}{\sqrt{2}}\right)t^{\alpha}. \tag{52}$$

Sequentially, we can compute the series $u_2(x,t)$ by assuming $n=2$ in the nth truncated error (46) such that

$$\begin{aligned}\mathscr{R}_j^2(x,t)&=\partial_t^{\alpha}u_2-\mu u_{2x}-6u_2u_{2x}^2\\&\quad-\left(3u_2^2-1\right)u_{2xx}+u_{2xxxx},\end{aligned} \tag{53}$$

where $u_2(x,t)=\tanh(x/\sqrt{2})+(\mu/\sqrt{2}\alpha)\operatorname{sech}^2(x/\sqrt{2})t^{\alpha}+(1/2\alpha^2)\mathscr{C}_2(x)t^{2\alpha}$. Then, by employing the conformable differential operator ∂_t^{α} on both sides of equation (53), we get that

$$\begin{aligned}\partial_t^{\alpha}\mathscr{R}_j^2(x,t)&=\mathscr{C}_2(x)-\mu\mathscr{C}_1'(x)-\mu\mathscr{C}_2'(x)\frac{t^{\alpha}}{\alpha}\\&\quad-\partial_t^{\alpha}\left(6u_2u_{2x}^2+\left(3u_2^2-1\right)u_{2xx}\right)\\&\quad+\mathscr{C}_1''(x)+\mathscr{C}_2''(x)\frac{t^{\alpha}}{\alpha}+\mathscr{C}_1^{(4)}(x)+\mathscr{C}_2^{(4)}(x)\frac{t^{\alpha}}{\alpha}.\end{aligned} \tag{54}$$

Now, solving the term $\partial_t^{\alpha}\mathscr{R}_j^2(x,t)_{|t=0}=0$ in the above equation with the help of Mathematica's symbolic architecture [51] leads to

$$\mathscr{C}_2(x)=-\mu^2\tanh\left(\frac{x}{\sqrt{2}}\right)\operatorname{sech}^2\left(\frac{x}{\sqrt{2}}\right). \tag{55}$$

Hence, the solution $u_2(x,t)$ can be given by

$$\begin{aligned}u_2(x,t)&=\tanh\left(\frac{x}{\sqrt{2}}\right)+\frac{\mu}{\sqrt{2}\alpha}\operatorname{sech}^2\left(\frac{x}{\sqrt{2}}\right)t^{\alpha}\\&\quad-\mu^2\tanh\left(\frac{x}{\sqrt{2}}\right)\operatorname{sech}^2\left(\frac{x}{\sqrt{2}}\right)\frac{t^{2\alpha}}{2\alpha^2}.\end{aligned} \tag{56}$$

Similarly, the truncated series $u_3(x,t)$ of the series expansion (44) can be calculate by assuming $n=3$ in (46), then, by solving the term $\partial^{2\alpha}\mathscr{R}_j^3(x,t)/\partial t^{2}{}_{|t=0}=0$ with the aid of Mathematica's symbolic architecture [51], we get

$$\mathscr{C}_3(x)=\frac{\mu^3}{\sqrt{2}}\left(\operatorname{Cosh}\left(\sqrt{2}x\right)-2\right)\operatorname{sech}^4\left(\frac{x}{\sqrt{2}}\right), \tag{57}$$

which reveals that $u_3(x,t)$ has the form

$$\begin{aligned}u_3(x,t)&=\tanh\left(\frac{x}{\sqrt{2}}\right)+\frac{\mu}{\sqrt{2}\alpha}\operatorname{sech}^2\left(\frac{x}{\sqrt{2}}\right)t^{\alpha}\\&\quad-\frac{\mu^2}{2\alpha^2}\tanh\left(\frac{x}{\sqrt{2}}\right)\operatorname{sech}^2\left(\frac{x}{\sqrt{2}}\right)t^{2\alpha}\\&\quad+\frac{\mu^3}{6\sqrt{2}\alpha^3}\left(\operatorname{Cosh}\left(\sqrt{2}x\right)-2\right)\operatorname{sech}^4\left(\frac{x}{\sqrt{2}}\right)t^{3\alpha}.\end{aligned} \tag{58}$$

Proceeding likewise, the solution $u_4(x,t)$ will have the form

$$\begin{aligned}u_4(x,t)&=\tanh\left(\frac{x}{\sqrt{2}}\right)+\frac{\mu}{\sqrt{2}\alpha}\operatorname{sech}^2\left(\frac{x}{\sqrt{2}}\right)t^{\alpha}\\&\quad-\frac{\mu^2}{2\alpha^2}\tanh\left(\frac{x}{\sqrt{2}}\right)\operatorname{sech}^2\left(\frac{x}{\sqrt{2}}\right)t^{2\alpha}\\&\quad+\frac{\mu^3}{6\sqrt{2}\alpha^3}\left(\operatorname{Cosh}\left(\sqrt{2}x\right)-2\right)\operatorname{sech}^4\left(\frac{x}{\sqrt{2}}\right)t^{3\alpha}\\&\quad-\frac{\mu^4}{48\alpha^4}\left(\sinh\left(\frac{3x}{\sqrt{2}}\right)-11\sinh\left(\frac{x}{\sqrt{2}}\right)\right)\operatorname{sech}^5\left(\frac{x}{\sqrt{2}}\right)t^{4\alpha}.\end{aligned} \tag{59}$$

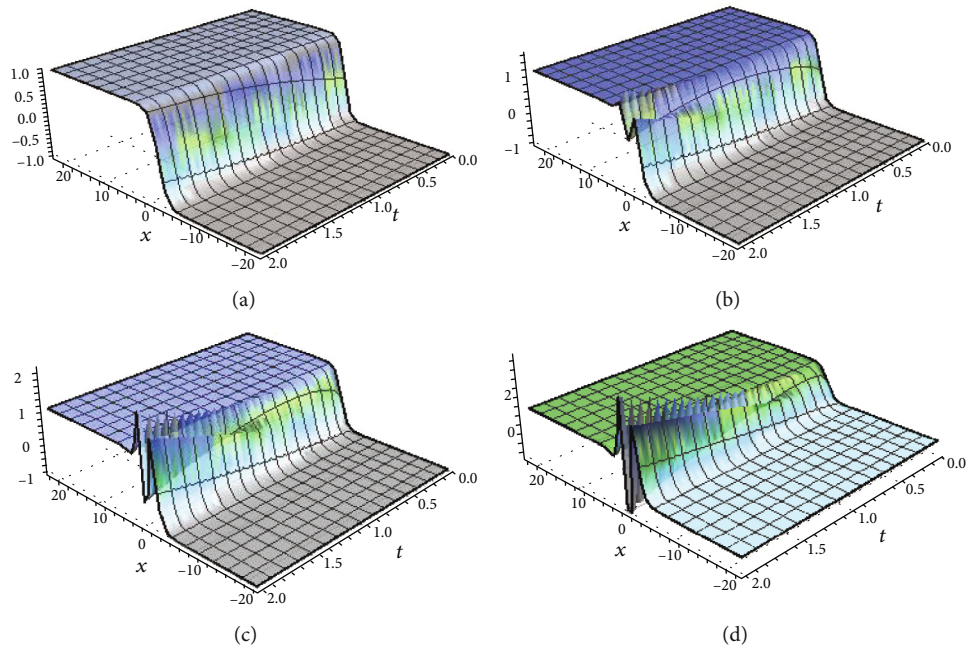

FIGURE 3: Surface wave behavior of $u_4(x,t)$ of the FCH4 model (40) and (41) with $\mu = 1$ for diverse α: (a) exact, (b) $\alpha = 0.75$, (c) $\alpha = 0.5$, and (d) $\alpha = 0.25$.

To close this method, it is assumed that $u_4(x,t)$ is an approximate solution, and $\mathscr{C}_n(x)$, $n \geq 5$ can be followed likewise. Later, by gathering the terms, $u(x,t)$ of the posed model (40) and (41) may be predicted. In particular, the solution of FCH4 equation (40) and (41) at $\alpha = 1$ and $\mu = 1$ can be written in the form

$$\begin{aligned} u(x,t) = {} & \tanh\left(\frac{x}{\sqrt{2}}\right) + \frac{1}{\sqrt{2}}\operatorname{sech}^2\left(\frac{x}{\sqrt{2}}\right)t \\ & - \frac{1}{2}\tanh\left(\frac{x}{\sqrt{2}}\right)\operatorname{sech}^2\left(\frac{x}{\sqrt{2}}\right)t^2 \\ & + \frac{1}{6\sqrt{2}}\left(\operatorname{Cosh}\left(\sqrt{2}x\right) - 2\right)\operatorname{sech}^4\left(\frac{x}{\sqrt{2}}\right)t^3 \\ & - \frac{1}{48}\left(\sinh\left(\frac{3x}{\sqrt{2}}\right) - 11\sinh\left(\frac{x}{\sqrt{2}}\right)\right) \\ & \cdot \operatorname{sech}^5\left(\frac{x}{\sqrt{2}}\right)t^4 + \cdots, \end{aligned} \tag{60}$$

which agrees with the analytical solution acquired by homotopy perturbation method (HPM) [25], q-HAM, and new iterative method (NIM) [24], so that

$$u(x,t) = \tanh\left(\frac{x+t}{\sqrt{2}}\right). \tag{61}$$

In the following, 3D graphical simulation of $u_4(x,t)$ of FCH4 model (40) and (41) with respect to different fractional parameter α are shown in Figure 3 for $\mu = 1$ over $[-20, 20] \times [0, 2]$. In Figure 4, 3D surface plots of FCH4 model (40) and (41) are depicted with fix $\alpha = 0.75$ versus μ such that $\mu = 1$ and $\mu = 0.75$ over the spatiotemporal domain $[-6, 6] \times [0, 3]$. Further, the obtained absolute errors $|u - u_4|$ are reported in Table 3 and compared to those results provided in [24] at $\mu = 1$ and $\alpha = 1$. The superiority of the present method follows from those results.

(i) Exponential wave solution of FCH4 equation

This segment is an attempt to gain an effective approximate solution to FCH4 equation (40) with the initial condition [24]

$$u(x,0) = e^{\lambda x}, \tag{62}$$

where λ is an arbitrary constant with $\lambda \neq 0$.

According the CFRS algorithm, the nth fractional series solution $u_n(x,t)$ of the FCH4 equation (40) about $t = 0$ in view of the initial condition (62) can be expressed as

$$u_n(x,t) = e^{\lambda x} + \sum_{i=1}^{n} \mathscr{C}_i(x)\frac{t^{i\alpha}}{\alpha^i i!}. \tag{63}$$

With the aid of the nth truncated error $\mathscr{R}_j^n(x,t)$ of (46), the unknown coefficients $\mathscr{C}_i(x)$ of the series expansion (63) can be computed for each value of $i = 1, 2, \cdots, n$. To achieve this goal, let the first fractional series solution of FCH4 equations (40) and (62) at $n = 1$ takes the form

$$u_1(x,t) = e^{\lambda x} + \frac{1}{\alpha}\mathscr{C}_1(x)t^{\alpha}. \tag{64}$$

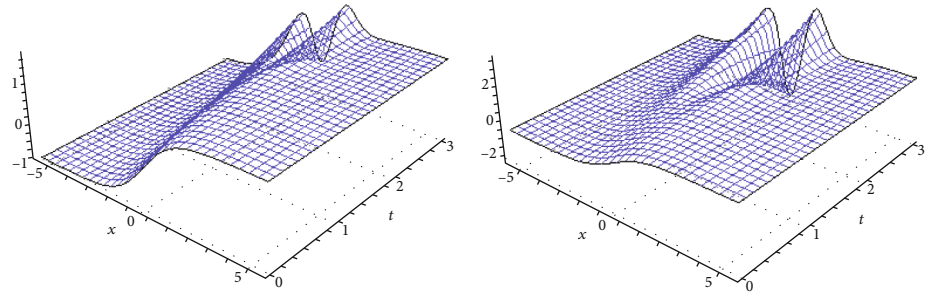

(a) (b)

Figure 4: Surface plots of FCH4 model (40) and (41) with fix $\alpha = 0.75$ versus μ: (a) $\mu = 1$ and (b) $\mu = 0.75$.

Table 3: Comparison of numerical results for FCH4 model (21)-(22) with $\lambda = 1$ and $\alpha = 1$.

t_i	x_i	$u(x,t)$	$u_4(x,t)$	$\lvert u - u_4\rvert$	$\lvert u - u_4\rvert\lvert u\rvert^{-1}$	**q-HAM** [24]	**NIM** [24]
0.01	0.0	0.007071	0.007071	2.35697×10^{-12}	3.33332×10^{-10}	2.356975×10^{-12}	1.151971×10^{-7}
	0.1	0.077625	0.077625	2.25475×10^{-12}	2.90466×10^{-11}	2.823765×10^{-10}	1.810671×10^{-7}
	0.2	0.147411	0.147411	1.96920×10^{-12}	1.33586×10^{-11}	5.749512×10^{-11}	6.167394×10^{-8}
	0.3	0.215758	0.215758	1.53980×10^{-12}	7.13667×10^{-12}	3.757261×10^{-11}	1.165205×10^{-9}
0.05	0.0	0.035341	0.035341	7.36197×10^{-9}	2.08315×10^{-7}	7.713501×10^{-8}	4.940148×10^{-5}
	0.1	0.105670	0.105670	7.00209×10^{-9}	6.62637×10^{-8}	1.124520×10^{-6}	8.990891×10^{-5}
	0.2	0.174958	0.174958	6.07535×10^{-9}	3.47246×10^{-8}	2.387229×10^{-7}	3.218897×10^{-5}
	0.3	0.242555	0.242555	4.70990×10^{-9}	1.94178×10^{-8}	1.516340×10^{-7}	4.548965×10^{-7}
0.08	0.0	0.056508	0.056508	7.71350×10^{-8}	1.36502×10^{-6}	7.361971×10^{-9}	1.306675×10^{-5}
	0.1	0.126596	0.126596	7.30464×10^{-8}	5.77003×10^{-7}	1.736922×10^{-7}	2.224480×10^{-5}
	0.2	0.195443	0.195443	6.30668×10^{-8}	3.22687×10^{-7}	3.622408×10^{-8}	7.794449×10^{-6}
	0.3	0.262415	0.262415	4.85727×10^{-8}	1.85099×10^{-7}	2.328496×10^{-8}	1.257660×10^{-7}
0.10	0.0	0.070593	0.070592	2.35226×10^{-7}	3.33214×10^{-6}	2.352262×10^{-7}	9.109940×10^{-5}
	0.1	0.140486	0.140486	2.22113×10^{-7}	1.58103×10^{-6}	2.722916×10^{-6}	1.740220×10^{-4}
	0.2	0.209006	0.209006	1.91136×10^{-7}	9.14497×10^{-7}	5.848640×10^{-7}	6.321236×10^{-5}
	0.3	0.275534	0.275534	1.46559×10^{-7}	5.31908×10^{-7}	3.686350×10^{-7}	8.108096×10^{-7}

Now, substitute $u_1(x,t)$ into $\mathcal{R}_j^1(x,t)$ and then solve $\mathcal{R}_j^1(x,t)_{|t=0} = 0$ to get

$$\mathcal{C}_1(x) = \lambda\left(\mu - \lambda\left(1 - 9e^{2\lambda x} + \lambda^2\right)\right)e^{\lambda x}. \tag{65}$$

Hence, the solution $u_1(x,t)$ is

$$u_1(x,t) = e^{\lambda x} + \frac{\lambda}{\alpha}\left(\mu - \lambda\left(1 - 9e^{2\lambda x} + \lambda^2\right)\right)e^{\lambda x}t^{\alpha}. \tag{66}$$

Sequentially, substitute $u_2(x,t)$ into the second truncated residual error $\mathcal{R}_j^2(x,t)$, apply the conformable operator ∂_t^{α} on both sides of the resulting equation, and solve $\partial_t^{\alpha}\mathcal{R}_j^2(x,t)_{|t=0} = 0$ with the aid of Mathematica's symbolic architecture [51] to get

$$\begin{aligned}\mathcal{C}_2(x) = \lambda^2\Big(&675\lambda^2 e^{4\lambda x} + \left(\lambda + \lambda^3 - \mu\right)^2 \\ &- 54\lambda\left(2\left(\lambda + 7\lambda^3\right) - \mu\right)e^{2\lambda x}\Big)e^{\lambda x},\end{aligned} \tag{67}$$

which implies that the second series solution is

$$\begin{aligned}u_2(x,t) = e^{\lambda x}\Bigg(&1 + \frac{\lambda}{\alpha}\left(\mu - \lambda\left(1 - 9e^{2\lambda x} + \lambda^2\right)\right)t^{\alpha} \\ &+ \frac{\lambda^2}{2\alpha^2}\Big(675\lambda^2 e^{4\lambda x} + \left(\lambda + \lambda^3 - \mu\right)^2 \\ &- 54\lambda\left(2\left(\lambda + 7\lambda^3\right) - \mu\right)e^{2\lambda x}\Big)t^{2\alpha}\Bigg).\end{aligned} \tag{68}$$

In the same fashion, the third and fourth series solutions of FCH4 equations (40) and (62) can be obtained successively as follows

$$\begin{aligned}u_3(x,t) = e^{\lambda x}\Big(1 + \frac{\lambda}{\alpha}\Big(\mu - \lambda\Big(1 - 9e^{2\lambda x} + \lambda^2\Big)\Big)t^{\alpha} \\ + \frac{\lambda^2}{2\alpha^2}\Big(675\lambda^2 e^{4\lambda x} + \big(\lambda + \lambda^3 - \mu\big)^2 \\ - 54\lambda\big(2\big(\lambda + 7\lambda^3\big) - \mu\big)e^{2\lambda x}\Big)t^{2\alpha} \\ + \frac{\lambda^3}{6\alpha^3}\Big(123039\lambda^3 e^{6\lambda x} \\ - 675\lambda^2\big(41\lambda + 713\lambda^3 - 15\mu\big)e^{4\lambda x} \\ + \big(\mu - \lambda\big(1 + \lambda^2\big)\big)^3 + 81\lambda\big(3\mu^2 - 12\mu\big(\lambda + 7\lambda^3\big) \\ + \lambda^2\big(13 + 194\lambda^2 + 757\lambda^4\big)\big)e^{2\lambda x}\Big)t^{3\alpha}\Big),\end{aligned} \tag{69}$$

$$\begin{aligned}u_4(x,t) = u_3(x,t) + \frac{\lambda^4}{24\alpha^4}\Big(972\lambda\big(\mu - 2\big(\lambda + 7\lambda^3\big)\big) \\ \cdot \big(\mu^2 - 4\mu\big(\lambda + 7\lambda^3\big) \\ + \lambda^2\big(5 + 82\lambda^2 + 365\lambda^4\big)\big)e^{2\lambda x} \\ + 1350\lambda^2\big(75\mu^2 - 10\lambda\mu\big(41 + 713\lambda^2\big) \\ + \lambda^2\big(613 + 22898\lambda^2 + 226477\lambda^4\big)\big)e^{4\lambda x} \\ - 15876\lambda^3\big(732\lambda + 23484\lambda^3 - 217\mu\big)e^{6\lambda x} \\ + 39110121\lambda^4 e^{8\lambda x} + \big(\lambda + \lambda^3 - \mu\big)^4\Big)e^{\lambda x}t^{4\alpha}.\end{aligned} \tag{70}$$

To close the process, we assume that $u_4(x,t)$ is the approximate solution. Following the same procedure, the values of $\mathscr{C}_n(x)$, $n \geq 5$ can be also computed. Thus, the expression of the series solution $u(x,t)$ of the FCH4 equation (40) along with condition (62) at $\alpha = 1$ and $\mu = 1$ can be written in the form

$$\begin{aligned}u(x,t) = e^{\lambda x}\Big(1 + \lambda\Big(1 - \lambda\Big(1 - 9e^{2\lambda x} + \lambda^2\Big)\Big)t \\ + \frac{\lambda^2}{2!}\Big(\big(\lambda + \lambda^3 - 1\big)^2 - 54\lambda\big(2\big(\lambda + 7\lambda^3\big) - 1\big)e^{2\lambda x} \\ + 675\lambda^2 e^{4\lambda x}\Big)t^2 + \frac{\lambda^3}{3!}\Big(123039\lambda^3 e^{6\lambda x} \\ - 675\lambda^2\big(41\lambda + 713\lambda^3 - 15\big)e^{4\lambda x} \\ + \big(1 - \lambda\big(1 + \lambda^2\big)\big)^3 + 81\lambda\Big(3 - 12\big(\lambda + 7\lambda^3\big) \\ + \lambda^2\big(13 + 194\lambda^2 + 757\lambda^4\big)\Big)e^{2\lambda x}\Big)t^3 \\ + \frac{\lambda^4}{4!}\Big(972\lambda\big(1 - 2\big(\lambda + 7\lambda^3\big)\big)\big(1 - 4\big(\lambda + 7\lambda^3\big) \\ + \lambda^2\big(5 + 82\lambda^2 + 365\lambda^4\big)\big)e^{2\lambda x} \\ + 1350\lambda^2\big(75 - 10\lambda\big(41 + 713\lambda^2\big) \\ + \lambda^2\big(613 + 22898\lambda^2 + 226477\lambda^4\big)\big)e^{4\lambda x} \\ - 15876\lambda^3\big(732\lambda + 23484\lambda^3 - 217\big)e^{6\lambda x} \\ + 39110121\lambda^4 e^{8\lambda x} + \big(\lambda + \lambda^3 - 1\big)^4\Big)t^4 + \cdots\Big).\end{aligned} \tag{71}$$

In the following, the 3D behaviors of surface wave function $u_4(x,t)$ of FCH4 model (40) and (62) are displayed in Figure 5 for the parameters $\mu = 1$ and $\lambda = -0.05$ with respect to $\alpha = 1$ and $\alpha = 0.75$ on $[-10, 10] \times [0, 1]$. While the fractional level curves of $u_3(x,t)$ for FCH4 model (40) and (62) are shown in Figure 6 compared to the third approximate solutions obtained in [24] for fix $t = 1$ on $[-15, 15]$ for various α values when $\lambda = -0.05$ and $\lambda = 0.05$. Error estimate for the third approximate solutions of FCH4 model (40) and (62) is provided in Table 4 by computing the absolute errors $|u_3 - u_{q\mathrm{HAM}}|$ and $|u_3 - u_{\mathrm{NIM}}|$ based on the results achieved by q-HAM and NIM [24] for $\alpha = 1$, $\mu = 1$, and $\lambda = 0.01$. From this comparison, it is evident that the results obtained by CFRS are in good agreement with those presented in the literature.

4.3. Solution of Nonlinear Sixth-Order Time-Fractional Cahn-Hilliard Equation. The one-dimensional nonlinear sixth-order fractional Cahn-Hilliard (FCH6) equation considered in this portion can be presented in terms of the conformable time derivative as follows [24]:

$$\begin{aligned}\partial_t^{\alpha} u = \mu u u_x - 18u u_{xx}^2 - 36u_x^2 u_{xx} - 24u u_x u_{xxx} \\ - \big(3u^2 - 1\big)u_{xxxx} + u_{xxxxxx},\end{aligned} \tag{72}$$

with the condition

$$u(x,0) = \tanh\left(\frac{x}{\sqrt{2}}\right), \tag{73}$$

$0 < \alpha \leq 1$, μ is a constant, $\mu \neq 0$, $x \in [a, b]$, $t \geq 0$, $u = u(x,t)$ is sufficiently differentiable function representing the wave-profile scaling spatiotemporal duration of wave propagation in dispersed media. Herein, the nonlinear terms in this model refer to chemical potential dynamics, and u_{xxxxxx} refers to wave scattering. This equation has applications in topology optimization, surface reconstruction, phase separation, phase ordering dynamics, magneto-acoustic propagation in plasma, multiphase incompressible fluid flows, image inpainting, and so forth [32].

According the CFRS algorithm, the nth fractional series solution $u_n(x,t)$ of the FCH6 equation (72) about $t = 0$ in view of the initial condition (73) can be expressed as

$$u_n(x,t) = \tanh\left(\frac{x}{\sqrt{2}}\right) + \sum_{i=1}^{n} \mathscr{C}_i(x)\frac{t^{i\alpha}}{\alpha^i i!}, \tag{74}$$

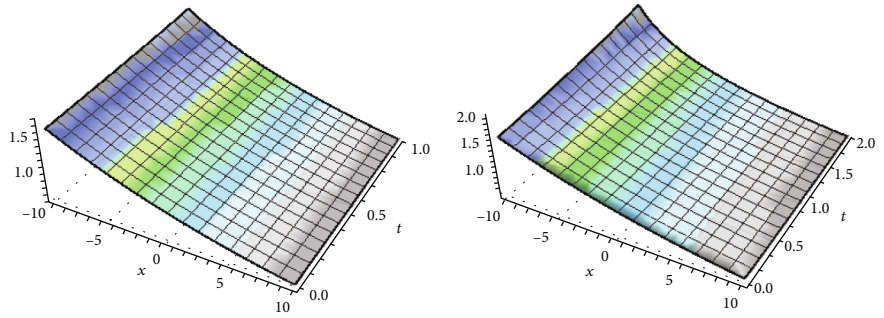

(a) (b)

Figure 5: Surface plots of FCH4 model (40)-(62) at $\mu = 1$ and $\lambda = -0.05$ for diverse α: (a) $\alpha = 1$ and (b) $\alpha = 0.75$.

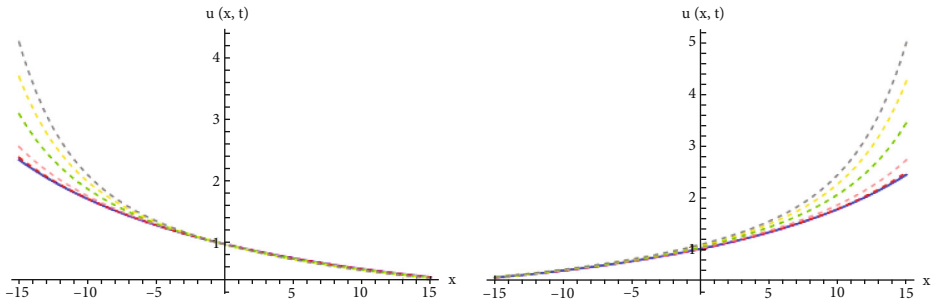

(a) (b)

Figure 6: Fractional level curves of $u_3(x,t)$ of FCH4 model (40) and (62) with $t = 1$ and $\mu = 1$: blue for q-HAM [24], red $\alpha = 1$, pink $\alpha = 0.75$, green $\alpha = 0.5$, yellow $\alpha = 0.25$, gray $\alpha = 0.1$; (a) $\lambda = -0.05$ and (b) $\lambda = 0.05$.

Table 4: Comparison of absolute errors of FCH4 model (40) and (62) with = 1,$\mu = 1$, and $\lambda = 0.01$.

t_i	$x = 1$		$x = 5$		$x = 20$	
	$\lvert u_3 - u_{qHAM}\rvert$	$\lvert u_3 - u_{NIM}\rvert$	$\lvert u_3 - u_{qHAM}\rvert$	$\lvert u_3 - u_{NIM}\rvert$	$\lvert u_3 - u_{qHAM}\rvert$	$\lvert u_3 - u_{NIM}\rvert$
0.5	8.8741×10^{-9}	7.7088×10^{-8}	1.0333×10^{-8}	8.7056×10^{-8}	1.8620×10^{-8}	1.4221×10^{-7}
1.0	7.0993×10^{-8}	6.1670×10^{-7}	8.2659×10^{-8}	6.9645×10^{-7}	1.4896×10^{-7}	1.1377×10^{-6}
1.5	2.3960×10^{-7}	2.0814×10^{-6}	2.7898×10^{-7}	2.3505×10^{-6}	5.0274×10^{-7}	3.8396×10^{-6}
2.0	5.6794×10^{-7}	4.9336×10^{-6}	6.6128×10^{-7}	5.5716×10^{-6}	1.1917×10^{-6}	9.1012×10^{-6}
2.5	1.1093×10^{-6}	9.6360×10^{-6}	1.2916×10^{-6}	1.0882×10^{-5}	2.3275×10^{-6}	1.7776×10^{-5}

and the residual error function $\mathcal{R}_\jmath(x,t)$ is

$$\begin{aligned}\mathcal{R}_\jmath(x,t) = {} & \partial_t^\alpha u - \mu u u_x + 18 u u_{xx}^2 + 36 u_x^2 u_{xx} \\ & + 24 u u_x u_{xxx} + \left(3u^2 - 1\right) u_{xxxx} \\ & - u_{xxxxxx}.\end{aligned} \tag{75}$$

For this purpose, the nth truncated error of $\mathcal{R}_\jmath(x,t)$ can be expressed in the form

$$\begin{aligned}\mathcal{R}_\jmath^n(x,t) = {} & \partial_t^\alpha u_n - \mu u_n u_{nx} + 18 u_n u_{nxx}^2 + 36 u_{nx}^2 u_{nxx} \\ & + 24 u_n u_{nx} u_{nxxx} + \left(3u_n^2 - 1\right) u_{nxxxx} \\ & - u_{nxxxxxx}.\end{aligned} \tag{76}$$

Thus, by minimizing the residual error (76) of the governing equation, the unknown coefficients $\mathcal{C}_i(x)$ of series expansion (74) for each value of $i = 1, 2, \cdots, n$ can be computed. Subsequently, the series solution at $n = 1$ has the form

$$u_1(x,t) = \tanh\left(\frac{x}{\sqrt{2}}\right) + \frac{1}{\alpha}\mathcal{C}_1(x) t^\alpha, \tag{77}$$

whereas the first residual function has the form

$$\begin{aligned}\mathcal{R}_\jmath^1(x,t) = {} & \partial_t^\alpha u_1 - \mu u_1 u_{1x} + 18 u_1 u_{1xx}^2 + 36 u_{1x}^2 u_{1xx} \\ & + 24 u_1 u_{1x} u_{1xxx} + \left(3u_1^2 - 1\right) u_{1xxxx} \\ & - u_{1xxxxxx}.\end{aligned} \tag{78}$$

Now, putting $u_1(x,t)$ into $\mathscr{R}_j^1(x,t)$ to get

$$\begin{aligned}\mathscr{R}_j^1(x,t) &= \mathscr{C}_1(x) - \frac{\mu}{\alpha^2}(\alpha\mathscr{C}_0(x) + \mathscr{C}_1(x)t^\alpha)\\ &\cdot \left(\alpha\mathscr{C}_0'(x) + \mathscr{C}_1'(x)t^\alpha\right)\\ &+ \frac{36}{\alpha^3}\left(\alpha\mathscr{C}_0'(x) + \mathscr{C}_1'(x)t^\alpha\right)^2\\ &\cdot \left(\alpha\mathscr{C}_0''(x) + \mathscr{C}_1''(x)t^\alpha\right)\\ &+ \frac{18}{\alpha^3}(\alpha\mathscr{C}_0(x) + \mathscr{C}_1(x)t^\alpha)\\ &\cdot \left(\alpha\mathscr{C}_0''(x) + \mathscr{C}_1''(x)t^\alpha\right)^2\\ &+ \frac{24}{\alpha^3}(\alpha\mathscr{C}_0(x) + \mathscr{C}_1(x)t^\alpha)\\ &\cdot \left(\alpha\mathscr{C}_0'(x) + \mathscr{C}_1'(x)t^\alpha\right)\\ &\cdot \left(\alpha\mathscr{C}_0^{(3)}(x) + \mathscr{C}_1^{(3)}(x)t^\alpha\right)\\ &+ \frac{3}{\alpha^3}(\alpha\mathscr{C}_0(x) + \mathscr{C}_1(x)t^\alpha)^2\\ &\cdot \left(\alpha\mathscr{C}_0^{(4)}(x) + \mathscr{C}_1^{(4)}(x)t^\alpha\right)\\ &- \frac{1}{\alpha}\left(\alpha\mathscr{C}_0^{(4)}(x) + \mathscr{C}_1^{(4)}(x)t^\alpha\right)\\ &- \frac{1}{\alpha}\left(\alpha\mathscr{C}_0^{(6)}(x) + \mathscr{C}_1^{(6)}(x)t^\alpha\right).\end{aligned} \tag{79}$$

By utilizing the fact $\mathscr{R}_j^1(x,t)_{|t=0} = 0$, it yields

$$\begin{aligned}&\mathscr{C}_1(x) + 36\mathscr{C}_0'(x)^2\mathscr{C}_0''(x) + \mathscr{C}_0(x)\\ &\cdot \left(18\mathscr{C}_0''(x)^2 - \mathscr{C}_0'(x)\left(\mu - 24\mathscr{C}_0^{(3)}(x)\right)\right)\\ &+ 3\mathscr{C}_0(x)^2\mathscr{C}_0^{(4)}(x) - \mathscr{C}_0^{(4)}(x) - \mathscr{C}_0^{(6)}(x) = 0,\end{aligned} \tag{80}$$

which implies that

$$\mathscr{C}_1(x) = \frac{\mu}{\sqrt{2}}\ \mathrm{sech}^2\left(\frac{x}{\sqrt{2}}\right)\tanh\left(\frac{x}{\sqrt{2}}\right). \tag{81}$$

Therefore, the solution $u_1(x,t)$ is

$$u_1(x,t) = \tanh\left(\frac{x}{\sqrt{2}}\right) + \frac{\mu}{\sqrt{2}\alpha}\ \mathrm{sech}^2\left(\frac{x}{\sqrt{2}}\right)\tanh\left(\frac{x}{\sqrt{2}}\right)t^\alpha. \tag{82}$$

Sequentially, the second truncated series $u_2(x,t)$ can be obtained by setting $n = 2$ in (76) such that

$$\begin{aligned}\mathscr{R}_j^2(x,t) &= \partial_t^\alpha u_2 - \mu u_2 u_{2x} + 18u_2u_{2xx}^2 + 36u_{2x}^2u_{2xx}\\ &+ 24u_2u_{2x}u_{2xxx} + \left(3u_2^2 - 1\right)u_{2xxxx}\\ &- u_{2xxxxxx},\end{aligned} \tag{83}$$

where $u_2(x,t) = \tanh(x/\sqrt{2}) + (\mu/\sqrt{2}\alpha)\ \mathrm{sech}^2(x/\sqrt{2})\tanh(x/\sqrt{2})t^\alpha + (1/2\alpha^2)\mathscr{C}_2(x)t^{2\alpha}$. By employing the operator ∂_t^α on both sides of equation (83), we get

$$\begin{aligned}\partial_t^\alpha\mathscr{R}_j^2(x,t) &= \mathscr{C}_2(x) - \mu\left(\mathscr{C}_0(x) + \mathscr{C}_1(x)\frac{t^\alpha}{\alpha} + \mathscr{C}_2(x)\frac{t^{2\alpha}}{2\alpha^2}\right)\\ &\cdot \left(\mathscr{C}_0'(x) + \frac{\mathscr{C}_1'(x)t^\alpha}{\alpha} + \frac{\mathscr{C}_2'(x)t^{2\alpha}}{2\alpha^2}\right)\\ &- \partial_t^\alpha\left(18u_2u_{2xx}^2 + 36u_{2x}^2u_{2xx}\right.\\ &+ 24u_2u_{2x}u_{2xxx} + \left(3u_2^2 - 1\right)u_{2xxxxx}\Big)\\ &- \mathscr{C}_0^{(6)}(x) - \frac{\mathscr{C}_1^{(6)}(x)t^\alpha}{\alpha} - \frac{\mathscr{C}_2^{(6)}(x)t^{2\alpha}}{2\alpha^2}.\end{aligned} \tag{84}$$

Solving the term $\partial_t^\alpha\mathscr{R}_j^2(x,t)_{|t=0} = 0$ with the aid of Mathematica's symbolic architecture [51] leads to

$$\begin{aligned}&\mathscr{C}_2(x) + 36\mathscr{C}_0'(x)\left(2\mathscr{C}_1'(x)\mathscr{C}_0''(x) + \mathscr{C}_0'(x)\mathscr{C}_1''(x)\right)\\ &+ \mathscr{C}_0(x)\left(36\mathscr{C}_0''(x)\mathscr{C}_1''(x) - \mathscr{C}_1'(x)\left(\mu - 24\mathscr{C}_0^{(3)}(x)\right)\right.\\ &+ 24\mathscr{C}_0'(x)\mathscr{C}_1^{(3)}(x)) - \mathscr{C}_1(x)\left(\mathscr{C}_0'(x)\left(\mu - 24\mathscr{C}_0^{(3)}(x)\right)\right.\\ &+ 6\left(3\mathscr{C}_0''(x)^2 + \mathscr{C}_0(x)\mathscr{C}_0^{(4)}(x)\right)\Big)\\ &- \mathscr{C}_1^{(4)}(x) + 3\mathscr{C}_0(x)^2\mathscr{C}_1^{(4)}(x) - \mathscr{C}_1^{(6)}(x) = 0,\end{aligned} \tag{85}$$

which implies that

$$\mathscr{C}_2(x) = \frac{\mu}{2}\zeta_1(x)\ \mathrm{sech}^4\left(\frac{x}{\sqrt{2}}\right)\tanh\left(\frac{x}{\sqrt{2}}\right), \tag{86}$$

in which $\zeta_1(x) = \mu(3 - \cosh(\sqrt{2}x)) - 3\sqrt{2}\ \mathrm{sech}^4(x/\sqrt{2})(249 - 163\cosh(\sqrt{2}x) + 8\cosh(2\sqrt{2}x))$.

Therefore, the series solution $u_2(x,t)$ can be given as

$$\begin{aligned}u_2(x,t) &= \tanh\left(\frac{x}{\sqrt{2}}\right) + \frac{\mu}{\sqrt{2}\alpha}\ \mathrm{sech}^2\left(\frac{x}{\sqrt{2}}\right)\tanh\left(\frac{x}{\sqrt{2}}\right)t^\alpha\\ &+ \frac{\mu}{4\alpha^2}\zeta_1(x)\ \mathrm{sech}^4\left(\frac{x}{\sqrt{2}}\right)\tanh\left(\frac{x}{\sqrt{2}}\right)t^{2\alpha}.\end{aligned} \tag{87}$$

Following the same procedure, the series $u_3(x,t)$ of (74) can be computed through setting $n = 3$ in (76) and solving the term $\partial^{2\alpha}\mathscr{R}_j^3(x,t)/\partial t^2{}_{|t=0} = 0$ to get $\mathscr{C}_3(x)$ as follows

$$\mathscr{C}_3(x) = \frac{\mu}{8}\zeta_2(x)\ \mathrm{sech}^6\left(\frac{x}{\sqrt{2}}\right)\tanh\left(\frac{x}{\sqrt{2}}\right), \tag{88}$$

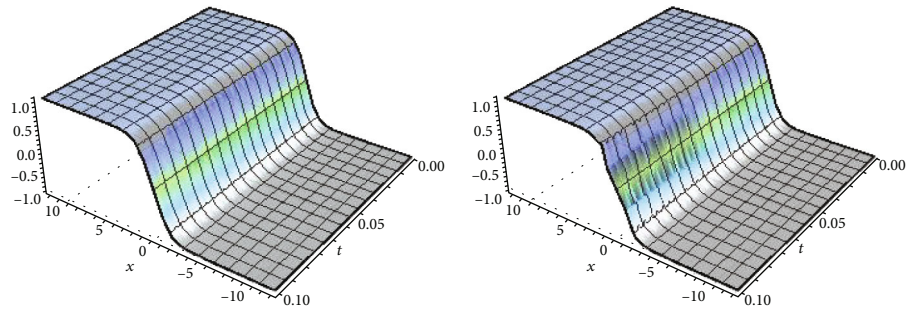

Figure 7: Surface wave behavior of $u_3(x,t)$ of FCH6 model (72) and (73) with $\mu = 0.01$ for diverse α: (a) $\alpha = 0.75$ and (b) $\alpha = 0.5$.

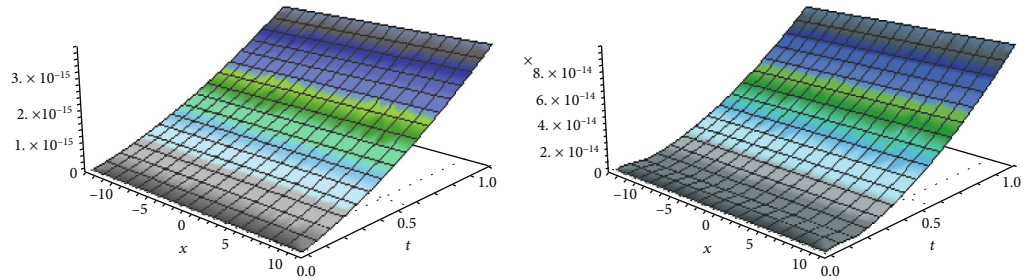

Figure 8: Surface of absolute error for FCH6 model (72) and (73) at $\mu = 0.01$ and $\alpha = 0.75$: (a) $|u_2 - u_{q\mathrm{HAM}}|$ and (b) $|u_2 - u_{\mathrm{NIM}}|$.

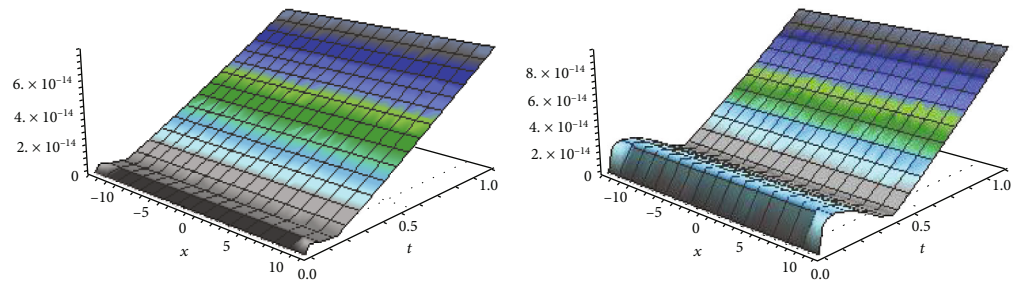

Figure 9: Surface of absolute error for FCH6 model (72) and (73) at $\mu = 0.01$ and $\alpha = 0.5$: (a) $|u_2 - u_{q\mathrm{HAM}}|$ and (b) $|u_2 - u_{\mathrm{NIM}}|$.

where

$$\begin{aligned}\zeta_2(x) = \sqrt{2}\mu^2\Big(&35 - 24\cosh\left(\sqrt{2}x\right) + \cosh\left(2\sqrt{2}x\right)\Big)\\ &- 18\sqrt{2}\Big(-28600273 + 33907584\cosh\left(\sqrt{2}x\right)\\ &- 7525233\cosh\left(2\sqrt{2}x\right) + 585152\cosh\left(3\sqrt{2}x\right)\\ &- 12286\cosh\left(4\sqrt{2}x\right) + 32\cosh\left(5\sqrt{2}x\right)\Big)\\ &\cdot\ \mathrm{sech}^8\left(\frac{x}{\sqrt{2}}\right) - 48\mu\Big(2499 - 96\cosh\left(\sqrt{2}x\right)\\ &- 20\Big(-89 + 184\cosh\left(\sqrt{2}x\right)\Big)\mathrm{sech}^4\left(\frac{x}{\sqrt{2}}\right)\Big),\end{aligned} \tag{89}$$

which implies that $u_3(x,t)$ has the form

$$\begin{aligned}u_3(x,t) = \tanh\left(\frac{x}{\sqrt{2}}\right) &+ \frac{\mu}{\sqrt{2}\alpha}\,\mathrm{sech}^2\left(\frac{x}{\sqrt{2}}\right)\tanh\left(\frac{x}{\sqrt{2}}\right)t^{\alpha}\\ &+ \frac{\mu}{4\alpha^2}\zeta_1(x)\,\mathrm{sech}^4\left(\frac{x}{\sqrt{2}}\right)\tanh\left(\frac{x}{\sqrt{2}}\right)t^{2\alpha}\\ &+ \frac{\mu}{48\alpha^3}\zeta_2(x)\,\mathrm{sech}^6\left(\frac{x}{\sqrt{2}}\right)\tanh\left(\frac{x}{\sqrt{2}}\right)t^{3\alpha}.\end{aligned} \tag{90}$$

To close the process, we suppose that $u_3(x,t)$ is the approximate solution. Then, $\mathscr{C}_n(x)$, $n \geq 4$, can be computed similarly. Anyhow, the n-term sequential solution can be written in the form $\mathscr{U}_n(x,t) = \sum_k^n u_k(x,t)$ as well as the solution $u(x,t)$ of the FCH6 equation (72) along

with condition (73) can be predicted as $u(x,t) = \lim_{n\longrightarrow\infty} \mathcal{U}_n(x,t)$.

In Figure 7, the behaviors of surface wave function $u_3(x,t)$ for FCH6 model (72) and (73) are presented in 3D with $\mu = 0.01$ for diverse α such that $\alpha = 0.75$ and $\alpha = 0.5$. While the surface plots of absolute error for FCH6 model (72) and (73) based on the results obtained in [24] at $\mu = 0.01$ are depicted in Figures 8 and 9 for $\alpha = 0.75$ and $\alpha = 0.5$, respectively. From these graphs, it is evident that the achieved results are in good agreement with those obtained in [24].

5. Concluding Remarks

In this paper, we have investigated the fractional parabolic partial differential models of Gardner and Cahn-Hilliard equations in conformable sense. Using the fractional residual method, the approximate solution has been successfully acquired of the posed problems without imposing any unsanctified restrictions. Numerical simulation has been carried out to highlight the ability of the suggested method. In this context, it can be concluded that the implemented approximation algorithm is a superior tool for computational purposes, it is computer oriented, it is relatively better compared to the existing numerical methods, and it is a straightforward and simple methodology that needs a few iterations to get accurate solutions. From the graphic representations, it is noticed that the solution behavior is harmonious for different fractional values and consistent with the integer value. In future work, multivariate series expansion based on residual error can be employed for multidimensional fractional evolution models in terms of the conformable derivative.

Data Availability

No data to be declared.

Conflicts of Interest

The authors declare that they have no conflicts of interest.

Authors' Contributions

All authors contributed equally to this article. They read and approved the final manuscript.

Acknowledgments

This work has been carried out during sabbatical leave granted to the author Mohammed Al-Smadi from Al-Balqa Applied University (BAU) during the academic year 2021/2022.

References

[1] M. Inc, A. Yusuf, A. I. Aliyu, and D. Baleanu, "Soliton solutions and stability analysis for some conformable nonlinear partial differential equations in mathematical physics," *Optical and Quantum Electronics*, vol. 50, article 190, 2018.

[2] D. Baleanu, M. Inc, A. Yusuf, and A. Aliyu, "Lie symmetry analysis, exact solutions and conservation laws for the time fractional Caudrey-Dodd-Gibbon-Sawada-Kotera equation," *Communications in Nonlinear Science and Numerical Simulation*, vol. 59, pp. 222–234, 2018.

[3] M. Al-Smadi, N. Djeddi, S. Momani, S. Al-Omari, and S. Araci, "An attractive numerical algorithm for solving nonlinear Caputo–Fabrizio fractional Abel differential equation in a Hilbert space," *Advances in Difference Equations*, vol. 2021, Article ID 271, 2021.

[4] S. Hasan, M. Al-Smadi, A. Freihet, and S. Momani, "Two computational approaches for solving a fractional obstacle system in Hilbert space," *Advances in Difference Equations*, vol. 2019, Article ID 55, 2019.

[5] E. Goncalves and D. Zeidan, "Numerical simulation of unsteady cavitation in liquid hydrogen flows," *Journal of Engineering Systems Modelling and Simulation*, vol. 9, no. 1, pp. 41–51, 2017.

[6] S. Kuila, T. R. Sekhar, and D. Zeidan, "On the Riemann problem simulation for the drift-flux equations of two-phase flows," *International Journal of Computational Methods*, vol. 13, no. 1, article 1650009, 2016.

[7] Z. Altawallbeh, M. Al-Smadi, I. Komashynska, and A. Ateiwi, "Numerical solutions of fractional systems of two-point BVPs by using the iterative reproducing kernel algorithm," *Ukrainian Mathematical Journal*, vol. 70, no. 5, pp. 687–701, 2018.

[8] J. Singh, "Analysis of fractional blood alcohol model with composite fractional derivative," *Chaos, Solitons & Fractals*, vol. 140, article 110127, 2020.

[9] B. Ghanbari, D. Kumar, and J. Singh, "An efficient numerical method for fractional model of allelopathic stimulatory phytoplankton species with Mittag-Leffler law," *Discrete & Continuous Dynamical Systems-S*, vol. 14, no. 10, pp. 3577–3587, 2021.

[10] O. Abu Arqub and M. Al-Smadi, "An adaptive numerical approach for the solutions of fractional advection- diffusion and dispersion equations in singular case under Riesz's derivative operator," *Physica A: Statistical Mechanics and its Applications*, vol. 540, article 123257, 2020.

[11] M. Alabedalhadi, M. Al-Smadi, S. Al-Omari, D. Baleanu, and S. Momani, "Structure of optical soliton solution for nonliear resonant space-time Schrödinger equation in conformable sense with full nonlinearity term," *Physica Scripta*, vol. 95, no. 10, article 105215, 2020.

[12] S. Hasan, M. Al-Smadi, H. Dutta, S. Momani, and S. Hadid, "Multi-step reproducing kernel algorithm for solving Caputo–Fabrizio fractional stiff models arising in electric circuits," *Soft Computing*, vol. 26, no. 8, pp. 3713–3727, 2022.

[13] D. G. Prakasha, P. Veeresha, and H. M. Baskonus, "Two novel computational techniques for fractional Gardner and Cahn-Hilliard equations," *Computational and Mathematical Methods*, vol. 1, no. 2, article e1021, 2019.

[14] O. S. Iyiola and O. G. Olayinka, "Analytical solutions of time-fractional models for homogeneous Gardner equation and non-homogeneous differential equations," *Ain Shams Engineering Journal*, vol. 5, pp. 999–1004, 2014.

[15] A. Atangana and D. Baleanu, "New fractional derivatives with non-local and non-singular kernel: theory and application to heat transfer model," https://arxiv.org/abs/1602.03408.

[16] B. Bira, T. R. Sekhar, and D. Zeidan, "Exact solutions for some time-fractional evolution equations using Lie group theory,"

Mathematical Methods in the Applied Sciences, vol. 41, no. 16, pp. 6717–6725, 2018.

[17] Z. Korpinar, M. Inc, D. Baleanu, and M. Bayram, "Theory and application for the time fractional Gardner equation with Mittag-Leffler kernel," *Journal of Taibah University for Science*, vol. 13, no. 1, pp. 813–819, 2019.

[18] M. Al-Smadi, S. Momani, N. Djeddi, A. El-Ajou, and Z. Al-Zhour, "Adaptation of reproducing kernel method in solving Atangana–Baleanu fractional Bratu model," *International Journal of Dynamics and Control*, vol. 10, 2022.

[19] D. Baleanu, Y. Ugurlu, M. Inc, and B. Kilic, "Improved (G'/G)-expansion method for the time-fractional biological population model and Cahn-Hilliard equation," *Journal of Computational and Nonlinear Dynamics*, vol. 10, no. 5, pp. 1–8, 2015.

[20] M. Al-Smadi and A. O. Abu, "Computational algorithm for solving Fredholm time-fractional partial integrodifferential equations of Dirichlet functions type with error estimates," *Applied Mathematics and Computation*, vol. 342, pp. 280–294, 2019.

[21] M. Al-Smadi, A. Freihat, H. Khalil, S. Momani, and R. A. Khan, "Numerical multistep approach for solving fractional partial differential equations," *International Journal of Computational Methods*, vol. 14, no. 3, article 1750029, 2017.

[22] H. Günerhan, H. Dutta, M. A. Dokuyucu, and W. Adel, "Analysis of a fractional HIV model with Caputo and constant proportional Caputo operators," *Chaos, Solitons & Fractals*, vol. 139, article 110053, 2020.

[23] M. Al-Smadi, H. Dutta, S. Hasan, and S. Momani, "On numerical approximation of Atangana-Baleanu-Caputo fractional integro-differential equations under uncertainty in Hilbert space," *Mathematical Modelling of Natural Phenomena*, vol. 16, p. 41, 2021.

[24] L. Akinyemi, O. S. Iyiola, and U. Akpan, "Iterative methods for solving fourth- and sixth-order time-fractional Cahn-Hillard equation," *Mathematical Methods in the Applied Sciences*, vol. 43, no. 7, pp. 4050–4074, 2020.

[25] A. Bouhassoun and M. H. Cherif, "Homotopy perturbation method for solving the fractional Cahn-Hilliard equation," *Journal of Interdisciplinary Mathematics*, vol. 18, no. 5, pp. 513–524, 2015.

[26] S. Qureshi, A. Yusuf, A. A. Shaikh, M. Inc, and D. Baleanu, "Fractional modeling of blood ethanol concentration system with real data application," *Chaos: An Interdisciplinary Journal of Nonlinear Science*, vol. 29, no. 1, article 013143, 2019.

[27] P. Veeresha, D. G. Prakasha, and S. Kumar, "A fractional model for propagation of classical optical solitons by using nonsingular derivative," *Mathematical Methods in the Applied Sciences*, vol. 43, 2020.

[28] M. Al-Smadi, "Fractional residual series for conformable time-fractional Sawada–Kotera–Ito, Lax, and Kaup–Kupershmidt equations of seventh order," *Mathematical Methods in the Applied Sciences*, vol. 44, 2021.

[29] H. Singh, A. K. Singh, R. K. Pandey, D. Kumar, and J. Singh, "An efficient computational approach for fractional Bratu's equation arising in electrospinning process," *Mathematical Methods in the Applied Sciences*, vol. 44, no. 13, pp. 10225–10238, 2021.

[30] M. Al-Smadi, O. Abu Arqub, and D. Zeidan, "Fuzzy fractional differential equations under the Mittag-Leffler kernel differential operator of the ABC approach: theorems and applications," *Chaos, Solitons & Fractals*, vol. 146, article 110891, 2021.

[31] A. Akgül, M. S. Hashemi, M. Inc, and S. A. Raheem, "Constructing two powerful methods to solve the Thomas–Fermi equation," *Nonlinear Dynamics*, vol. 87, no. 2, pp. 1435–1444, 2017.

[32] Y. Li, D. Jeong, H. Kim, C. Lee, and J. Kim, "Comparison study on the different dynamics between the Allen-Cahn and the Cahn-Hilliard equations," *Computers & Mathematics with Applications*, vol. 77, no. 2, pp. 311–322, 2019.

[33] M. Inc, "On numerical soliton solution of the Kaup-Kupershmidt equation and convergence analysis of the decomposition method," *Applied Mathematics and Computation*, vol. 172, no. 1, pp. 72–85, 2006.

[34] N. K. Tripathi, S. Das, S. H. Ong, H. Jafari, and M. M. Al Qurashi, "Solution of time-fractional Cahn-Hilliard equation with reaction term using homotopy analysis method," *Advances in Mechanical Engineering*, vol. 9, no. 12, 2017.

[35] G. Akagi, G. Schimperna, and A. Segatti, "Fractional Cahn-Hilliard, Allen-Cahn and porous medium equations," *Journal of Differential Equations*, vol. 261, no. 6, pp. 2935–2985, 2016.

[36] M. Ran and X. Zhou, "An implicit difference scheme for the time-fractional Cahn-Hilliard equations," *Mathematics and Computers in Simulation*, vol. 180, pp. 61–71, 2021.

[37] H. Liu, A. Cheng, H. H. Wang, and J. Zhao, "Time-fractional Allen-Cahn and Cahn-Hilliard phase-field models and their numerical investigation," *Computers & Mathematics with Applications*, vol. 76, no. 8, pp. 1876–1892, 2018.

[38] A. Arafa and G. Elmahdy, "Application of residual power series method to fractional coupled physical equations arising in fluids flow," *International Journal of Differential Equations*, vol. 2018, Article ID 7692849, 10 pages, 2018.

[39] K. Hosseini, A. Bekir, M. Kaplan, and O. Guner, "On a new technique for solving the nonlinear conformable time-fractional differential equations," *Optical and Quantum Electronics*, vol. 49, no. 11, p. 343, 2017.

[40] H. Jafari, H. Tajadodi, N. Kadkhoda, and D. Baleanu, "Fractional subequation method for Cahn-Hilliard and Klein-Gordon equations," *Abstract and Applied Analysis*, vol. 2013, Article ID 587179, 5 pages, 2013.

[41] M. Al-Smadi, O. Abu Arqub, and M. Gaith, "Numerical simulation of telegraph and Cattaneo fractional-type models using adaptive reproducing kernel framework," *Mathematical Methods in the Applied Sciences*, vol. 44, no. 10, pp. 8472–8489, 2021.

[42] M. Al-Smadi, O. Abu Arqub, and S. Momani, "Numerical computations of coupled fractional resonant Schrödinger equations arising in quantum mechanics under conformable fractional derivative sense," *Physica Scripta*, vol. 95, no. 7, article 075218, 2020.

[43] A. Atangana, D. Baleanu, and A. Alsaedi, "New properties of conformable derivative," *Open Mathematics*, vol. 13, no. 1, pp. 889–898, 2015.

[44] M. Al-Smadi, O. Abu Arqub, and S. Hadid, "An attractive analytical technique for coupled system of fractional partial differential equations in shallow water waves with conformable derivative," *Journal of Applied Mathematics and Computing*, vol. 72, no. 8, article 085001, 2020.

[45] R. Khalil, M. Al Horani, A. Yousef, and M. Sababheh, "A new definition of fractional derivative," *Journal of Computational and Applied Mathematics*, vol. 264, pp. 65–70, 2014.

[46] T. Abdeljawad, "On conformable fractional calculus," *Journal of computational and Applied Mathematics*, vol. 279, pp. 57–66, 2015.

[47] M. Al-Smadi, O. Abu Arqub, and S. Hadid, "Approximate solutions of nonlinear fractional Kundu-Eckhaus and coupled fractional massive Thirring equations emerging in quantum field theory using conformable residual power series method," *Physica Scripta*, vol. 95, no. 10, article 105205, 2020.

[48] D. R. Anderson and D. J. Ulness, "Newly defined conformable derivatives," *Advances in Dynamical Systems and Applications*, vol. 10, pp. 109–137, 2015.

[49] C. Chen and Y. Jiang, "Simplest equation method for some time-fractional partial differential equations with conformable derivative," *Computers & Mathematics with Applications*, vol. 75, no. 8, pp. 2978–2988, 2018.

[50] Q. Feng, "A new approach for seeking coefficient function solutions of conformable fractional partial differential equations based on the Jacobi elliptic equation," *Chinese Journal of Physics*, vol. 56, no. 6, pp. 2817–2828, 2018.

[51] Wolfram Research, Inc, *Mathematica Edition: Version 12.2*, Wolfram Research, Champaign, IL, 2020.